Natural disturbances from bark beetle outbreaks and windthrow increasingly affect Europe's most mature and carbon-rich forests.

Simon Besnard[1], Alba Viana-Soto[2], Henrik Hartmann[3,4,5], Marco Patacca[6,7], Viola H.A. Heinrich[1,8], Katja Kowalski[2], Maurizio Santoro[9], Wanda De Keersmaecker[10], Ruben Van De Kerchove[10], Martin Herold[1], Cornelius Senf[2]

[1]GFZ Helmholtz Centre for Geosciences, Telegrafenberg, 14473 Potsdam, Germany

[2]Technical University of Munich, School of Life Sciences, Earth Observation for Ecosystem Management, Freising, Germany

[3]Julius Kühn Institute (JKI) - Federal Research Centre for Cultivated Plants, Institute for Forest Protection, Quedlinburg, Germany.

[4]Faculty of Forest Sciences and Forest Ecology, Georg-August-University, Büsgenweg 5, 37077 Göttingen, Germany

[5]Department of Biogeochemical Processes, Max Planck Institute for Biogeochemistry, Hans Knoell Str. 10, 07745 Jena, Germany

[6]Sustainable Forest Ecosystems, Wageningen Environmental Research, Wageningen, The Netherlands

[7]Forest Ecology and Forest Management Group, Wageningen University and Research, Wageningen, The Netherlands

[8]School of Geographical Sciences, University of Bristol, Bristol, United Kingdom

[9]Gamma Remote Sensing, 3073 Gümligen, Switzerland

[10]Environmental Intelligence, Flemish Institute for Technological Research (VITO), Mol, Belgium

Correspondence to: Simon Besnard (simon.besnard@gfz.de)

Abstract. Europe's forests store nearly 40 PgC and provide a critical carbon sink of ~0.2 PgC yr^{-1}, yet climate-sensitive disturbances increasingly threaten this capacity. Although disturbance rates from windthrow and bark beetle outbreaks have risen in recent decades, it remains unclear whether these events increasingly affect the oldest and largest trees, which store a disproportionate share of carbon. Focusing on bark beetle outbreaks and windthrow, the dominant natural disturbance agents in temperate and boreal European forests, we combine three decades of satellite-derived disturbance maps with spatially explicit data on forest age, biomass, and species composition to reveal patterns of structural selectivity across Europe. We show that natural disturbances have shifted toward older, carbon-rich forest patches, with disturbed forest area >60 years old nearly tripling since 2010 (from 0.38 to 1.06 Mha). This pattern reflects a qualitative shift in disturbance dynamics, from historically episodic, wind-dominated impacts to increasingly persistent, climate-amplified bark beetle outbreaks that preferentially affect mature spruce forests in Central Europe (effect size = 1.1). As a result, biomass losses from natural disturbances in spruce forests increased fivefold between the early (2011-2016) and recent (2017-2023) periods, outpacing the expansion of the disturbed area. Trend-based projections indicate that, if current patterns of structural selectivity persist, natural disturbances could expose biomass carbon stocks equivalent to approximately 20% of Europe's contemporary forest carbon sink by 2040 (~0.05 PgC yr^{-1} or ~0.8 PgC cumulative). Our findings reveal a previously unquantified structural

susceptibility: climate-sensitive disturbances increasingly affect forest structures with high per-hectare carbon stocks, amplifying disturbance-related carbon susceptibility and weakening the long-term effectiveness of Europe's forest carbon sink. Adaptive management strategies that promote structural and compositional diversification in high-risk regions will be critical to stabilise forest carbon storage under continued climate change.

1 Introduction

European forests are central to the continent's climate mitigation efforts, storing nearly 40 PgC in aboveground and soil carbon pools and acting as a net carbon sink of ~0.2 PgC per year between 2010 and 2019 (Pan et al., 2024). Yet, this sink is weakening. A large share of Europe's forests originated from post-war planting campaigns and are entering maturity, during which carbon accumulation slows as stands approach saturation (Nabuurs et al., 2013). At the same time, harvest levels have remained high or increased in recent decades (Turubanova et al., 2023), and climate-driven natural disturbances (e.g., windthrow and bark beetle outbreaks) are intensifying across the region (Seidl and Senf, 2024). These pressures are particularly concerning for structurally mature forests dominated by large, old trees, which store a disproportionate share of carbon and sustain long-term sequestration (Besnard et al., 2025).

We define disturbances broadly as either natural or anthropogenic in origin. Natural disturbances are events triggered by environmental agents such as windstorms and bark beetle outbreaks (including associated salvage logging), whereas harvest refers to timber removal directly driven by management. Natural disturbances have become more frequent and severe in recent decades (Patacca et al., 2023), coinciding with reports of declining forest carbon sinks in parts of Europe (Migliavacca et al., 2025; Ritter et al., 2025). Since 2018, bark beetle outbreaks have surpassed windthrow as the dominant natural cause of canopy loss (Patacca et al., 2023) (Fig. S1), especially in Central Europe (Austria, Germany, Czechia, and parts of northern Italy), where compound droughts and heatwaves have predisposed spruce to infestation, resulting in unprecedented mortality ("Living with bark beetles," 2019; Weynants et al., 2024). Warming further accelerates bark beetle reproduction (Wermelinger and Seifert, 1999), enabling multiple generations per year (Jakoby et al., 2019) and facilitating outbreaks at higher elevations (Hartmann et al., 2025) and more northerly latitudes ("Korhonen K. T., Ahola A. et al. (2021) Forests of Finland 2014-2018 and their development 1921-2018," n.d.; "Pulgarin Diaz J. A., Melin M. et al. (2024) Relationship between stand and landscape attributes and *Ips typographus* salvage loggings in Finland," n.d.). These trends are likely to persist as climate change continues. Although beetles dominate today, periodic windstorms have historically caused losses, and future storms could again shift disturbance dynamics, as seen with events such as windstorms Vivian and Wiebke (in 1990), Lothar and Martin (in 1999), and Klaus (in 2009).

Despite extensive documentation of disturbance extent and trends across Europe (Ceccherini et al., 2020; Hansen et al., 2013; Turubanova et al., 2023; Viana-Soto and Senf, 2025) (Fig. S2), the structural characteristics of affected forests, especially their age and biomass, remain poorly quantified at a continental scale. Recent work has shown that aboveground

biomass losses across Europe accelerated markedly after 2018, with a disproportionate rise in biomass loss per unit disturbed area in temperate forests (Kowalski et al., 2026), yet the structural basis of this decoupling remains unresolved. Local studies suggest that older, high-biomass forest patches may be particularly vulnerable to natural disturbances (Brockerhoff et al., 2008; Neuner et al., 2015); yet it remains unclear whether disturbances show systematic structural selectivity at continental scales. Susceptibility likely depends on both species composition and structural heterogeneity, with homogeneous forest patches offering continuous host connectivity that facilitates the spread of disturbance (Raffa et al., 2008). The critical question is whether rising disturbance rates reflect a simple increase in the total area affected or a systematic shift toward structurally vulnerable forest cohorts, and how this selectivity may reshape Europe's forest carbon dynamics. Answering this is essential not only for anticipating demographic and carbon trajectories but also for improving Earth system models, which often represent disturbances stochastically or without structural constraints (Bergkvist et al., 2025; Calle and Poulter, 2021; O'Sullivan et al., 2024).

~~Here, we present the first continental assessment of structural and compositional selectivity in recent forest disturbances across Europe.~~Here, we present the first continental assessment of structural and compositional selectivity in bark beetle and windthrow disturbances across European temperate and boreal forests. Integrating three decades of satellite-derived disturbance maps (Viana-Soto and Senf, 2025) with spatially explicit data on forest age (Besnard et al., 2021~~, n.d.~~), aboveground biomass (Santoro and Cartus, 2025), and genus ~~composition~~group (De Keersmaecker et al., 2024), we ask whether natural disturbances are increasingly affecting older, carbon-dense forests and how these patterns differ across three ~~functional groups~~genus groups: spruce, other needleleaf, and broadleaf species. We quantify shifts in the age and biomass structure of disturbed forest patches, test whether impacts concentrate in structurally homogeneous forests, and project how continued structural selectivity may increase the susceptibility of forest carbon stocks to disturbance through 2040. Our findings indicate that Europe's forest carbon sink is becoming increasingly vulnerable not only because disturbance rates are rising, but also because disturbances are disproportionately affecting forest areas with high carbon stocks.

2 Materials and Methods

2.1 Annual disturbance data resampling

To generate spatially consistent disturbance layers across Europe, we resampled annual disturbance maps from the European Forest Disturbance Atlas v2.1.1 dataset (Viana-Soto and Senf, 2025) to a 100 m grid (EPSG: 4326) aligned with the ESA CCI biomass dataset v6 (Santoro and Cartus, 2025). EFDA provides annual maps indicating, for each 30 m pixel, whether a disturbance occurred (binary 0/1) and the associated agent (harvest, wind/bark beetle, fire, mixed).

We first reprojected each annual EFDA layer to EPSG:4326. The reprojected 30 m binary disturbance maps were aggregated to 100 m resolution using average resampling. Within each 100 m pixel (~10,000 m²), we computed the fraction of overlapping 30 m sub-pixels (~9 m² each) classified as disturbed, yielding a continuous disturbance fraction rather than a

binary indicator. This approach preserves information on sub-pixel heterogeneity and yields, for each 100 m pixel, the proportion of forested area disturbed by a given agent in a given year.

To account for known commission errors (Viana-Soto and Senf, 2025) in the disturbance maps for 2018 and 2023 over northern latitudes, we excluded all disturbance values for these two years in areas north of 65°N. This filtering step mitigates the influence of artefact-driven expansions in the boreal region. Fire and mixed disturbances were excluded from this study because our research question specifically concerns the structural consequences of the documented shift from wind-dominated to bark beetle-dominated disturbance regimes (Patacca et al., 2023; Senf and Seidl, 2021). Such a shift unfolds through biotic and abiotic mechanisms distinct from fire dynamics and is geographically concentrated in temperate and boreal forest systems. We focus on two disturbance categories: harvest, representing planned timber removal for wood production or silvicultural reasons, and wind and bark beetle disturbances, representing unplanned canopy loss driven by natural agents but often followed by human management (i.e. salvage logging). We use the term disturbance broadly throughout to encompass both categories, as both human timber removal and natural canopy loss are disturbances with ecological consequences, while maintaining a consistent distinction between natural disturbances and harvest in all analyses and figures.

The final dataset consists of harmonised, agent-specific disturbance-fraction layers at 100 m resolution for the period 1985-2023. These layers are spatially aligned with the forest age and biomass data used in downstream analyses, ensuring consistent pixel-level integration across all data streams.

2.2 Genus map data resampling

To incorporate tree species composition into the analysis, we ~~downscaled~~aggregated the 10 m European genus classification map (De Keersmaecker et al., 2024) (EPSG:3035) to a 100 m grid in EPSG:4326, ensuring consistency with the forest age, biomass, and disturbance datasets. The map distinguishes eight classes: Larix, Picea, Pinus, Fagus, Quercus, other needleleaf, other broadleaf, and no-tree. Prior to spatial aggregation, these eight classes were reclassified at the native 10 m resolution into three ~~functional~~genus groups based on known differences in disturbance susceptibility: spruce (Picea spp.), other needleleaf (Larix spp., Pinus spp., and other conifers), and broadleaf (Fagus spp., Quercus spp., and other broadleaf species). Non-tree pixels were assigned to nodata at this stage and excluded from the subsequent majority filter. Spruce was retained as a distinct group given its documented preferential susceptibility to bark beetle outbreaks (Hlásny et al., 2021; Berthelot et al., 2021) and its dominant role in Central European disturbance dynamics (Seidl et al., 2016a). This grouping is analytical and is not intended to provide a balanced comparison across taxa. The reclassified 10 m map was then reprojected to EPSG:4326 and aggregated to 100 m resolution using a mode-based majority filter, assigning each 100 m cell the ~~functional~~genus group that occurred most frequently among its underlying 10 m pixels. Reclassifying to three

~~functional~~genus groups prior to spatial aggregation reduces class fragmentation during the majority filter, producing more robust and stable genus group assignments under the projection transformation from EPSG:3035 to EPSG:4326.

This procedure preserves the dominant ~~functional~~genus group signal while reducing spatial detail to the scale of the biomass and disturbance layers. The resulting 100 m genus group map is fully aligned with the European forest domain and all other gridded datasets used in subsequent analyses. Assigning a single dominant ~~functional~~genus group to each 100 m pixel may underrepresent compositional heterogeneity, particularly in structurally complex mixed forests. Results should therefore be interpreted as reflecting the dominant compositional signal of each pixel rather than its full taxonomic complexity.

2.3 Integration of the different Earth Observation data streams

To build a unified dataset for analysis, we first identified all forested pixels that experienced either harvest or natural disturbances (windthrow or bark beetle) between 1985 and 2023, as mapped in the European Forest Disturbance Atlas v2.1.1. For every disturbed 100 m pixel (in EPSG:4326), we extracted co-located forest structural and compositional attributes.

Each disturbed pixel was associated with:

1. The annual disturbance fraction for each agent (harvest, windthrow and bark beetle), derived from the EFDA v2.1.1 at 100 m resolution in EPSG:4326 (Viana-Soto and Senf, 2025),
2. forest age from the GAMIv3.0 ensemble (Besnard et al., 2021), provided as 20 independent realisations at 100 m resolution, with all analyses fixed to the 2010 estimate ,
3. aboveground biomass from the ESA CCI biomass v6.0 ensemble (Santoro and Cartus, 2025), provided as 20 independent realisations at 100 m resolution for the year 2010, converted to carbon using a factor of 0.47,
4. forest fraction within each 100 m pixel, derived from the EFDA v2.1.1 forest mask at 100 m resolution (Viana-Soto and Senf, 2025), and
5. the dominant ~~functional group class~~genus group (spruce, other needleleaf, or broadleaf), resampled from the 10 m European genus classification map (De Keersmaecker et al., 2024) following the reclassification and aggregation procedure described in Section 2.2.

The resulting dataset is stored in tabular format, with each row corresponding to a single forested pixel that was disturbed at least once between 1985 and 2023. Disturbance records prior to 2011 are retained in the dataset for trend-based forecasting (Section 2.7) but are not used in the structural selectivity analyses, which are restricted to the 2011-2023 period.

2.4 Temporal analyses of disturbed forest age structure

To assess whether the age structure of disturbed forests changed over time, we examined shifts in the 2010 baseline forest age of pixels affected by harvest or natural disturbances. Using the harmonised disturbance dataset (2011-2023), we selected all 100 m pixels with ≥30% forest fraction. A minimum forest fraction of 30% was applied to exclude pixels dominated by non-forest land cover while retaining partially forested cells representative of Europe's fragmented forest landscapes. This threshold was chosen to balance the exclusion of predominantly non-forested pixels against retention of the mixed land cover conditions typical of European agricultural-forest mosaics. ~~A minimum forest fraction of 30% was applied to exclude pixels dominated by non-forest land cover while retaining partially forested cells representative of Europe's fragmented forest landscapes.~~We retained only those where ≥50% of the forested area was disturbed by a specific agent in a given year. A minimum disturbance fraction of 50% was applied to focus the analysis on high-severity, largely stand-replacing events where structural attributes of the disturbed stand are most meaningfully characterised. This conservative threshold minimises the influence of partial disturbances. All analyses were fixed to the 2010 age estimate regardless of the year of disturbance. This design choice is intentional: by holding the landscape age structure constant, we ensure that differences in the age of disturbed stands between the early (2011-2016) and recent (2017-2023) periods reflect actual changes in disturbance selectivity rather than the confounding effect of natural forest ageing. Any shift toward older disturbed cohorts, therefore, represents an actual change of forest age classes preferentially affected by disturbances, independent of natural stand development.

We acknowledge that pixels experiencing a stand-replacing disturbance in the early period would, if disturbed again in the recent period, be assigned an age that no longer reflects their true post-disturbance condition. However, recurrent stand-replacing natural disturbance events were found in less than 3% of all forested pixels across the study domain (Table S3), consistent with the long return intervals documented for European forest disturbances (Schelhaas et al., 2003; Seidl et al., 2014). Furthermore, stands regenerating after a stand-replacing event in the early period would not reach the structural maturity required to become susceptible to bark beetle attack or windthrow within a 12-year window, given known minimum canopy development trajectories in European forests (Lindegaard et al., 2016; Suvanto et al., 2025). Together, these considerations confirm that repeat natural disturbance events do not substantially affect our continental-scale conclusions. The proportion of pixels experiencing two or more harvest events within the study period was higher (~8%), reflecting shorter rotation cycles compared to natural disturbance return intervals. Although this proportion is modest, repeated harvest events in the same pixel do not alter the fixed 2010 biomass baseline used in the analysis and are therefore unlikely to systematically bias the harvest-related structural comparisons between periods. However, results for harvest should be interpreted with this caveat, especially in regions characterised by short rotation forestry.

We aggregated all pixel-level information onto a 100 km-diameter hexagonal grid to increase robustness in regional comparisons. For each hexagon and disturbance type, we calculated the median 2010 age of disturbed pixels for the early

(2011-2016) and recent (2017-2023) periods. Differences between periods indicated whether disturbances increasingly affected older or younger forests, independent of stand development.

To quantify changes in the full age distribution, we used the energy distance (ED) metric (Rizzo and Székely, 2016), which measures divergence between two probability distributions and is sensitive to both shifts in central tendency and distributional shape. ED measures distributional divergence between the age structures of disturbed forests in the two periods: higher energy distance values indicate that the age distributions of disturbed forests in the early and recent periods are more dissimilar, reflecting a greater shift in the structural cohorts targeted by disturbance. ED between the early and recent periods was computed for each hexagon and disturbance type:

$$ED(X, Y) = 2 * E[||X - Y||] - E[||X - X'||] - E[||Y - Y'||] \quad \text{Eq. (1)}$$

Where X and Y represent the 2010 age distributions of disturbed pixels in the early and recent periods. X′ and Y′ are additional independent random samples drawn from the same distributions as X and Y, respectively, used to normalise the expected distance. $\|\cdot\|$ denotes the Euclidean distance.

To complement age-based analyses, we evaluated how the joint distribution of forest age and aboveground biomass (AGB) changed across disturbance types and periods. Disturbed pixels were binned into a 7×7 matrix of age and biomass classes for each period (e.g. 0-20, 21-40, ..., >120 years or MgC ha^{-1}), and the fraction of pixels in each structural class was computed to form two-dimensional disturbance density matrices. Matrix differences (recent minus early) highlight which structural cohorts gained or lost prominence in recent disturbances.

Given known ecological thresholds (e.g., bark beetles preferentially affecting spruce > ~60 years) (Hlásny et al., 2021), we further grouped stands into broad age classes (1-60 years, > 60 years) and computed annual fractions disturbed in each class. For all metrics, we summarised uncertainty across all 20 realisations of the forest age ensembleusing medians and 5th-95th percentiles. Temporal trajectories were visualised separately for natural disturbances and harvests. These analyses enabled us to determine whether disturbances increasingly targeted older and/or higher-biomass landscapes, and whether these structural shifts differed between natural disturbances and harvest activities.

2.5 ~~Functional~~Genus-group-specific biomass loss assessment

To investigate ~~functional~~ group-specific susceptibility to disturbance, we assessed the structural and cumulative biomass loss across three genus groups: Spruce, Other needleleaf (including *Larix*, *Pinus*, and other conifers), and Broadleaf (including *Fagus*, *Quercus*, and other broadleaf species). The analysis focused on harvests and natural disturbances (wind and bark beetles) across two periods: 2011-2016 and 2017-2023. For each disturbed pixel, we used ensemble median aboveground biomass estimates (converted to carbon using a factor of 0.47), forest fraction, genus ~~class~~group, and disturbance fraction.

For all analyses, aboveground biomass was fixed to the 2010 ESA CCI v6.0 estimate, consistent with the fixed 2010 forest age baseline. This approach ensures that differences in the biomass of disturbed stands between the early and recent periods reflect changes in disturbance selectivity rather than background biomass accumulation across the landscape. Biomass values were filtered to remove non-positive and extreme outliers (IQR-based filtering). Cohen's d effect sizes were calculated to quantify shifts in biomass distribution between early and recent periods within each genus group. To assess total biomass loss, we aggregated disturbed biomass by multiplying per-pixel biomass by forest fraction, pixel area, and disturbance fraction, and then summing across all pixels within each genus and period. This was repeated across the 20 independent realisations of the ESA CCI biomass ensemble to derive ensemble medians and uncertainty bounds (5^{th}-95^{th} percentiles). The resulting values were expressed in terragrams of carbon (TgC). Together, these analyses provide a quantitative view of how biomass loss from disturbances varies by ~~species~~genus group and whether structural shifts or total loss intensified in the more recent period.

2.6 Assessing structural homogeneity in disturbed forests

To determine whether natural disturbances increasingly affect structurally homogeneous forested landscapes, we quantified spatial and temporal changes in structural variability using the coefficient of variation (CV) of aboveground biomass (MgC ha^{-1}). Biomass CV was calculated as a proxy for landscape-level structural heterogeneity. Data preparation, spatial filtering, and hexagonal grid aggregation followed the same procedure described in Section 2.3. For each hexagon, CV values were computed separately for each of the 20 independent realisations of the ESA CCI biomass ensemble; hexagons with fewer than 50 valid disturbed pixels were excluded. It is important to note that CV computed at the 100 km hexagon scale reflects landscape-level variability in biomass across multiple stands and forest types, rather than within-stand structural complexity. It should therefore be interpreted as a proxy for the degree of structural uniformity across the disturbance-prone landscape mosaic, rather than a direct measure of stand-level heterogeneity.

Structural heterogeneity was compared between early (2011-2016) and recent (2017-2023) disturbance periods. Analyses were stratified by disturbance type and by ~~forest~~ genus group (spruce, other needleleaf, broadleaf). Differences between periods were quantified using Cohen's *d* and mapped as ΔCV (recent minus early). To assess continuous shifts, we computed the annual median CV of pre-disturbance biomass across all retained hexagons separately for each of the 20 biomass ensemble members, then derived the annual ensemble median and 5th-95th percentile range across members, yielding a temporal trajectory of structural heterogeneity with associated uncertainty bounds. For each disturbance type and genus, we fitted ordinary least-squares regressions of CV against year; slopes and significance levels summarised long-term changes in structural heterogeneity. Temporal coherence between harvest- and disturbance-related CV trajectories was evaluated using Pearson's r.

2.7 Trend-based forecasts of biomass susceptibility through 2040

Spatial aggregation and disturbance quantification: Data preparation, spatial filtering, and hexagonal grid aggregation followed the same procedure described in Section 2.3. This filtering captures high-severity, stand-replacing events, where most of the canopy is affected, and therefore produces conservative disturbance estimates that underrepresent low-severity or partial disturbances. Aboveground biomass values from the ESA CCI v6.0 ensemble (20 realisations) were converted to carbon using a factor of 0.47. Median biomass per hexagon, disturbance type, and period was used in subsequent simulations.

Annual disturbed area and biomass susceptibility: For each disturbance type and year, we computed the total disturbed forest area per hexagon as:

$$A_{i,y} = f_{i,y} * d_{i,y} * a_i \quad \text{Eq. (2)}$$

Where $f_{i,y}$ is the forest fraction in pixel i and year y, $d_{i,y}$ is the disturbance fraction in pixel i and year y, and a_i is the area of pixel i (converted to Mha). The total disturbed area for each year and disturbance agent was obtained by summing $A_{i,y}$ across all pixels within a hexagon. This produced an annual time series of total disturbed area per hexagon from 1985 to 2023, which was used as input for forecasting.

Trend-based forecasting and model selection: To reduce short-term noise, annual disturbance trajectories were smoothed using a centred 5-year moving average. Model fitting was restricted to recent periods (2008-2023, or 2015-2023 in sensitivity tests) to capture contemporary disturbance dynamics. For each hexagon and disturbance agent, we fit two candidate models to the smoothed series: (i) linear increase and (ii) exponential decay, and selected the best model using the Akaike Information Criterion (AIC). Decay models were constrained to plausible decreasing trends, reflecting potential stabilisation after outbreak peaks. Linear models represented continued intensification. The selected model was then used to forecast areas of disturbance for 2024-2040.

Uncertainty estimation via Taylor's law: To account for heteroskedasticity in disturbance dynamics, we applied Taylor's law (Taylor, 1961) separately to natural disturbances and harvest. For each hexagon, we computed the mean and variance of annual disturbed area over the model-fitting window (2008-2023; or 2015-2023 in sensitivity tests). These mean-variance pairs were then pooled across all hexagons and fit with a log-log linear regression, yielding global parameters a and b:

$$\mathrm{Var}(A_y) = a * \mu_y^{\,b} \quad \text{Eq. (3)}$$

Where $Var(A_y)$ is the variance of the annual disturbed area in year y, μ_y is the mean yearly disturbed area in year y, and a and b are regression parameters estimated from historical data. Projected variances for 2024-2040 were derived using the predicted means and this relationship.

Mean-variance pairs were then reparameterised into lognormal distributions, from which we drew 1,000 Monte Carlo realisations per hexagon and year. This captures the heavy-tailed distribution of disturbance activity, allowing extreme but infrequent disturbance pulses to appear in the forecasts (Senf et al., 2025).

Biomass susceptibility simulation: For each Monte Carlo simulation and year, forecasted disturbed areas were converted to carbon susceptibility by multiplying them by biomass values sampled from two composition-specific scenarios:

- Early scenario: biomass distribution of forests disturbed during 2011-2016
- Recent scenario: biomass distribution of forests disturbed during 2017-2023

Here, biomass carbon susceptibility is defined as the amount of aboveground carbon stock affected by disturbance and therefore conditionally vulnerable to future carbon loss under the two disturbance-biomass scenarios. For every hexagon and biomass ensemble member, a biomass value was drawn from the scenario distribution and multiplied by the simulated disturbed area. This produced a time series of biomass susceptibility per hexagon, year, and disturbance type across 1,000 simulations. Results were aggregated across ensemble members, simulations, and hexagons to compute per-year medians and 5th-95th percentiles at both the hexagon and pan-European scales. This framework links area-based disturbance forecasts with uncertainty in biomass composition, providing scenario-explicit estimates of future carbon susceptibility.

3 Results

3.1 Shift in disturbance susceptibility toward older, high-biomass forests.

Satellite-based observations revealed an increase in age selectivity since 2017, with natural disturbances disproportionately affecting older and more carbon-dense forests. The area disturbed annually in forests >60 years old nearly tripled between early (2011-2016) and recent (2017-2023) periods, rising from 0.38 Mha to 1.06 Mha, while disturbances in younger forests increased more modestly from 0.35 to 0.56 Mha (Table S1). This shift is most evident in the joint distribution of forest age and aboveground carbon stocks: recent disturbances increasingly concentrate in landscapes exceeding both 60 years and 80 MgC ha^{-1} (Fig. 1a,c). The most substantial biomass losses occurred in mature spruce forests in Central and Eastern Europe (Fig. S5a, c).

Natural disturbances showed greater distributional shifts (median ED: 1.5 years; 5th-95th percentile: 1.0-2.3) than harvests (median: 0.9 years; 5th-95th percentile: 0.6-1.3), with peak values in Central and Eastern Europe (Fig. 2a). Critically, this structural change was directional: 64% of grid cells showed increases in the median age of disturbed landscapes (Fig. 2c), and the concentration of values above the 1:1 line in Fig. 2d confirms that recent disturbances systematically targeted older cohorts.

Regional patterns revealed substantial heterogeneity in this continental trend. In Western and Central Europe, disturbances after 2017 were increasingly concentrated in landscapes older than 60 years (Fig. S4c,e), consistent with compound drought-amplified bark beetle dynamics in spruce-dominated regions. Northern Europe showed comparatively stable age distributions, with younger forested landscapes remaining dominant, though gradual ageing was evident (Fig. S4a). In Eastern and Southeastern Europe, disturbances more frequently affected forests ≤60 years old, particularly 40-50-year-old monospecific pine and spruce plantations, a pattern consistent with high stem densities and drought stress in even-aged landscapes.

In contrast to natural disturbances, harvest patterns showed structural stability. Harvests remained concentrated in older stands (>60 years) but typically targeted lower-biomass forests than those affected by natural disturbances (Fig. 1b, d; Fig. S3b, d). While harvested area increased substantially (from 4.93 to 6.75 Mha), the age and biomass distributions shifted only modestly (median ED: 0.9 years), with slight increases in mid-aged stands (60-100 years; 40-80 MgC ha^{-1}) likely reflecting salvage operations in beetle-affected regions (Fig. 2b).

The contrast between stable harvest selectivity and shifting bark beetle and windthrow patterns suggests that climate-amplified biotic agents, rather than management changes, drive the observed structural selectivity within the disturbance types and geographic regions captured by our analysis.

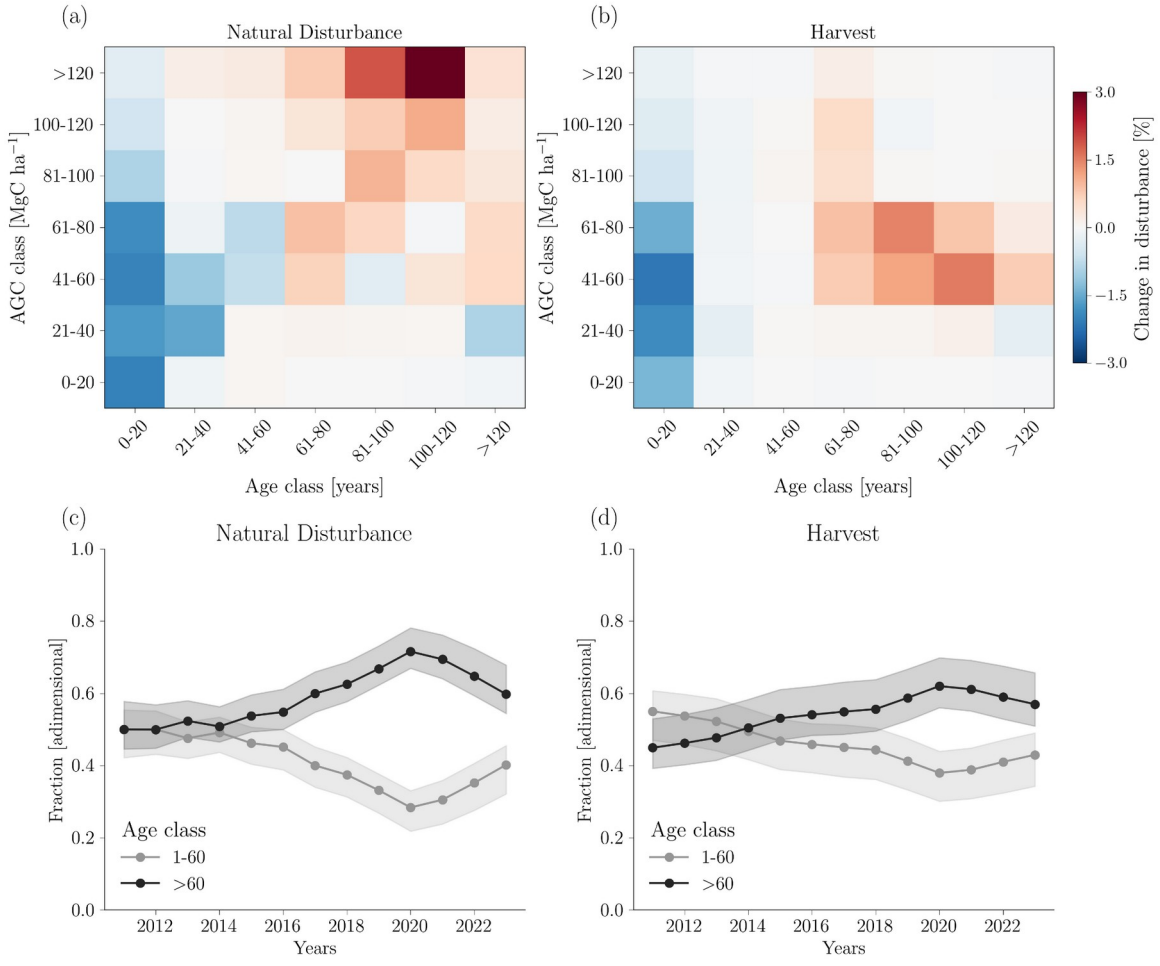

Figure 1: Structural characteristics of forests affected by natural disturbances and harvest across Europe. (a-b) Change in the fraction of disturbed forests between 2017-2023 and 2011-2016 across combinations of aboveground carbon (AGC) class (Mg C ha^{-1}) and forest age class (years). Biomass values reflect 2010 ESA CCI v6.0 estimates fixed prior to any disturbance within the study period. –Age classes refer to the 2010 baseline age of each pixel, not the age at the time of disturbance. Warmer colours (reds) indicate increased disturbance in that class; cooler colours (blues) indicate a decline. (c-d) Temporal evolution of the fraction of disturbed area by forest age class (1-60 years vs. >60 years) for natural disturbances (c) and harvest (d) from 2011 to 2023. Shaded ribbons represent the 95% quantile range across the 20-member forest age ensemble, and lines show the median trajectory. Only 100 m pixels with at least 30% forest cover were retained, and among those, only pixels where at least 50% of the forested area was disturbed by a specific agent in a given year were considered.

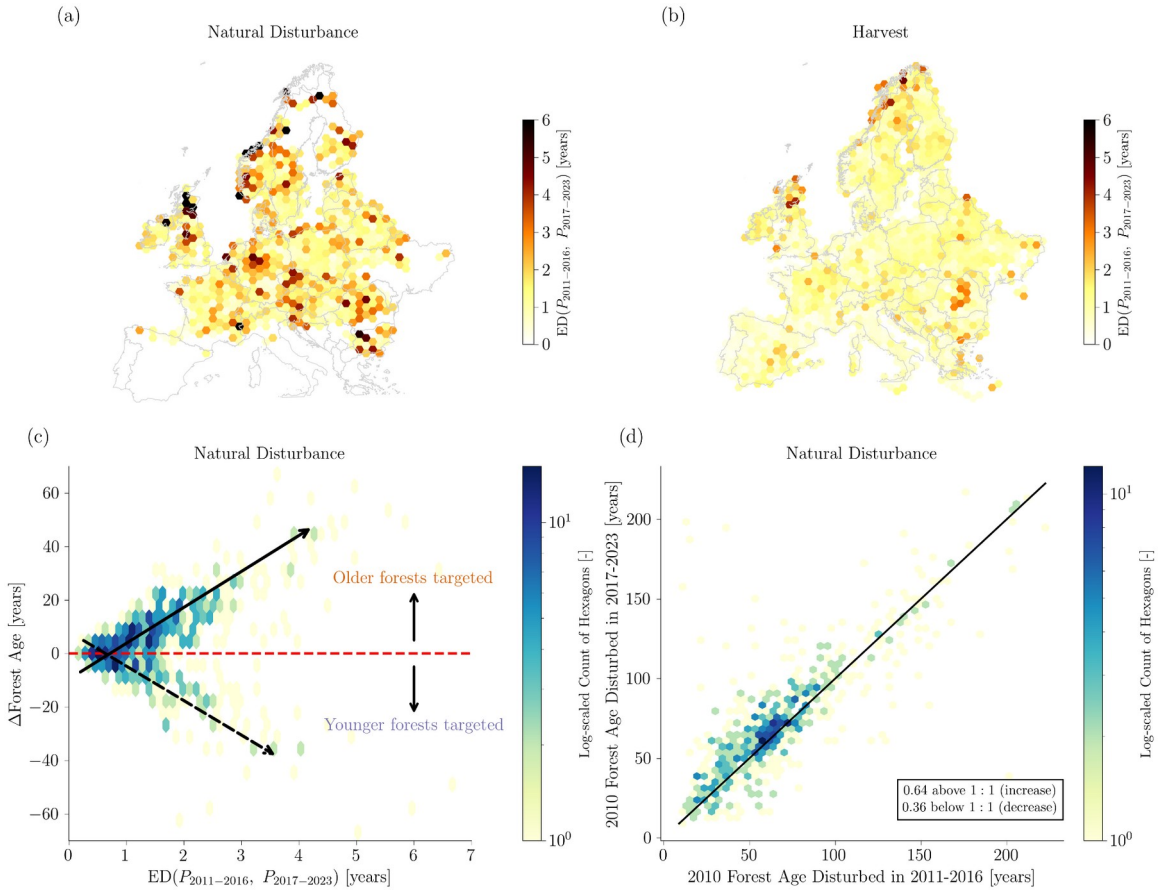

Figure 2: Structural changes in disturbed forest stands over time, quantified with the energy distance metric. (a-b) Spatial distribution of energy distance values comparing forest age distributions affected by natural disturbances (a) and harvest (b) between two periods (2011-2016 vs. 2017-2023). Higher values indicate greater temporal dissimilarity in the age of disturbed forests. (c) Relationship between ED and the direction of structural change (ΔForest Age). Because all ages are fixed to 2010 values, the differences reflect selection, not regrowth or mortality. Positive Δ values indicate a shift toward forest disturbance, specifically a growing tendency to affect older forest patches in later periods, independent of natural forest ageing. (d) Comparison of the 2010 baseline forest age for disturbances occurring in 2011-2016 (x-axis) and 2017-2023 (y-axis). Values above the 1:1 line indicate that forests disturbed in the later period were generally older than those disturbed earlier, while values below the line reflect a shift toward younger forest patches. Only 100 m pixels with at least 30% forest cover were retained, and among those, only pixels where at least 50% of the forested area was disturbed by a specific agent in a given year were considered. Hexagons with fewer than 50 valid pixels per period were excluded from analysis. Each hexagon has a diameter of approximately 100 km. Hexagons were used as aggregation units because they offer equal-distance neighbour relationships and minimise edge effects compared to squares.

3.2 High-biomass spruce forest patches are disproportionately affected by natural disturbances.

Spruce-dominated forests exhibited the strongest structural shift in disturbance impacts, with natural disturbances increasingly concentrated in high-biomass forest patches during the period 2017-2023 (Fig. 3; Fig. S5). Biomass carbon losses from natural disturbances in spruce forests increased nearly fivefold between periods, from 11.5 TgC (5th-95th percentile: 9.4-13.9) in 2011-2016 to 62.3 TgC (51.9-74.4) in 2017-2023. This increase outpaced the sixfold expansion in disturbed area (from 0.07 to 0.46 Mha; Table S2), indicating a disproportionate rise in carbon losses relative to disturbance extent.

This disproportionate increase reflects a systematic shift toward higher-biomass cohorts. Median biomass of disturbed spruce forest patches rose from approximately 75 to 95 MgC ha^{-1} between periods (Cohen's d = 1.1, indicating a large effect; Fig. 3a,c), demonstrating that recent disturbances increasingly affected structurally mature spruce forests. The spatial concentration of this shift in Central Europe (Fig. S5a), where high-biomass spruce monocultures are prevalent, further highlights the role of forest structure in amplifying disturbance-related carbon impacts.

Together, expanding disturbance extent and increasing per-hectare biomass resulted in a disproportionate increase in carbon losses from spruce forests. Although spruce accounted for approximately 44 % of the total naturally disturbed area in the recent period, it contributed approximately 52 % of natural-disturbance-related biomass carbon losses. This contrasts sharply with other forest types. In other coniferous and broadleaf forests, biomass losses from natural disturbances increased more gradually, from 18.0 to 38.5 TgC (+114 %)and from 16.1 to 18.0 TgC (+12 %), respectively (Fig. 3c). These increases closely tracked expansions in disturbed area (0.30 to 0.58 Mha in other conifers; 0.23 to 0.27 Mha in broadleaves) and were not accompanied by significant shifts in the biomass structure of affected forest patches (median biomass stable; effect sizes < 0.5; Fig. 3a).

Harvest-related biomass losses also increased across all forest types (Fig. 3d), but in contrast to natural disturbances, these trends were driven almost entirely by expanding harvested area rather than by structural selectivity. Harvested area expanded from 0.78 to 1.63 Mha in spruce and from 2.41 to 3.26 Mha in other needleleaf forests, while broadleaf harvested area remained stable (1.47 to 1.49 Mha), and the biomass distribution of harvested forest patches remained stable (Fig. 3b). Consequently, most harvest-related biomass losses originated from other needleleaf (121.4 and 169.7 TgC in 2011-2016 and 2017-2023, respectively) and broadleaf forests (76.3 and 73.3 TgC), with spruce contributing a smaller but increasing share (47.2 and 101.7 TgC). This contrast underscores that the disproportionate increase in carbon losses observed in spruce forests arises primarily from climate-sensitive natural disturbances interacting with forest structure, rather than from shifts in management practices.

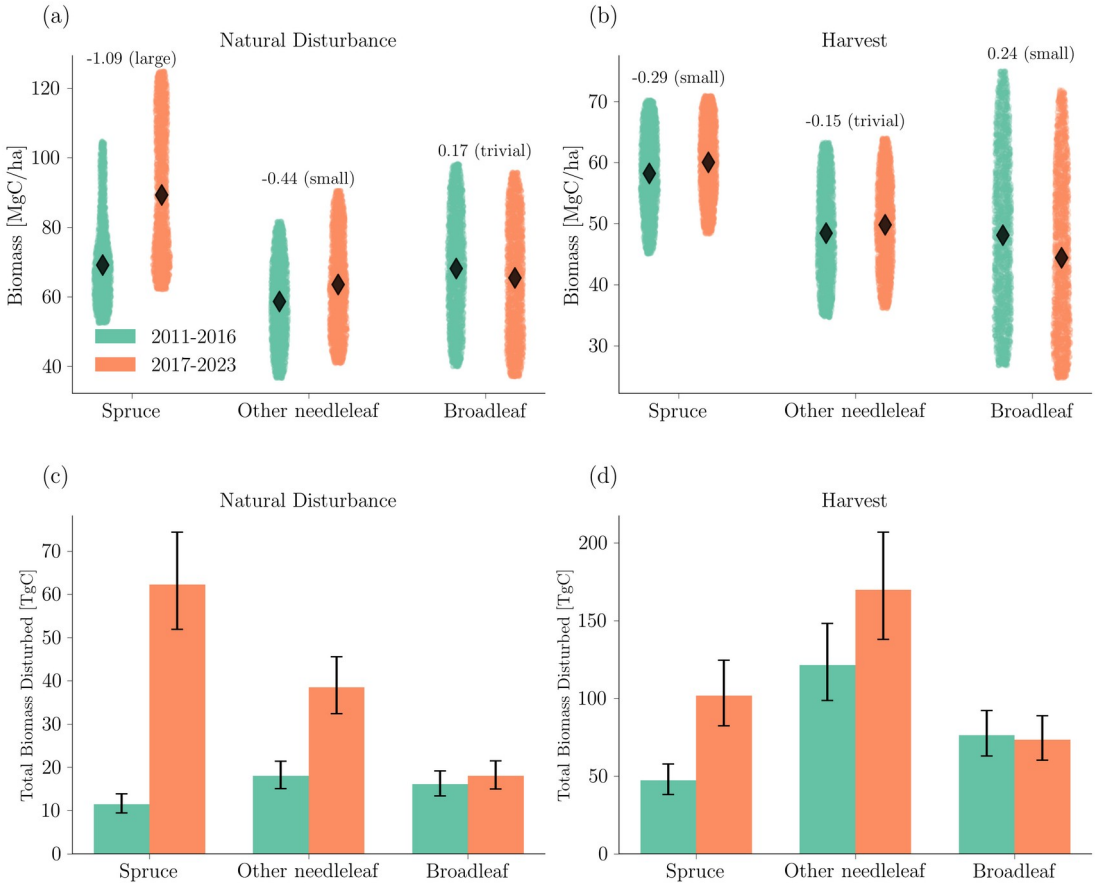

Figure 3: Structural and quantitative changes in aboveground carbon loss by ~~species~~genus group for natural forest disturbances and harvests. (a-b) Median biomass of disturbed ~~forest~~ forest patches by dominant tree genus for natural disturbances (a) and harvest (b), comparing early (2011-2016) and recent (2017-2023) periods. Biomass values reflect 2010 ESA CCI v6.0 estimates fixed prior to any disturbance within the study period. Each point in the jitter plots represents a pixel. Annotated values represent Cohen's d effect sizes, quantifying the standardised difference in median biomass between periods for each ~~species~~genus group. (c-d) Total AGB loss (TgC) by ~~species~~genus group from natural disturbances (c) and harvest (d) in both periods. Bars indicate the median across a 20-member biomass ensemble, and error bars represent the 5th and 95th percentiles, capturing uncertainty in biomass estimates. Only 100 m pixels with at least 30% forest cover were retained, and among those, only pixels where at least 50% of the forested area was disturbed by a specific agent in a given year were considered.

3.3 Natural disturbances increasingly occur in structurally homogeneous landscapes.

Beyond targeting older, high-biomass forests, natural disturbances are increasingly concentrated in structurally homogeneous forest patches. Between 2011-2016 and 2017-2023, natural disturbances shifted markedly toward such stands, as indicated

by declining coefficients of variation (CV) in pre-disturbance biomass, particularly in Central and Eastern Europe (Fig. 4a). By contrast, harvest-related CV changes were spatially diffuse and lacked the geographic clustering characteristic of climate-sensitive bark beetle outbreaks (Fig. 4b).

This shift toward homogeneous forest patches was strongly genus-specific (Fig. 4c). Spruce-dominated landscapes exhibited a pronounced decline in CV (Cohen's d = 1.18), indicating that recent disturbances targeted structurally uniform spruce forests. This effect size is large, larger even than the shift toward high-biomass forest patches (Section 3.2; d = 1.1), and suggests that structural homogeneity may be as crucial as stand age in determining bark beetle susceptibility. By contrast, broadleaf (Cohen's d = 0) and other needleleaf forests (Cohen's d = 0.24) showed no to weak declines, confirming that the homogeneity signal is driven by spruce monocultures in Central Europe.

The shift toward structurally homogeneous forest patches was not only a snapshot difference between periods but an ongoing temporal trend. In spruce forests, the CV of pre-disturbance biomass declined significantly over time in both naturally disturbed (slope = -0.0051 yr^{-1}, p = 0.03) and harvested (slope = -0.0048 yr^{-1}, p = 0.01) forest patches, equivalent to a reduction of approximately 0.06 CV units (~20% relative to the 2011 baseline) over the 2011-2023 period (Fig. 4d). Remarkably, natural disturbances and harvests showed nearly identical downward trajectories (Pearson's r = 0.84), suggesting both agents increasingly target the same structurally uniform forest patches, likely reflecting salvage operations following bark beetle infestations. The temporal coupling between natural disturbance and harvest area trajectories was similarly strong (Pearson's r = 0.75), consistent with salvage operations driving the harvest signal. By contrast, broadleaf and other needleleaf forests showed no significant temporal trends in CV (Fig. S6b,c), and the strong spruce signal dominated the continental-scale average. Across all genera, harvested forest patches consistently exhibited higher CV than naturally disturbed forest patches (Pearson's r = 0.90), consistent with the interpretation that natural disturbances disproportionately affect the most homogeneous forests.

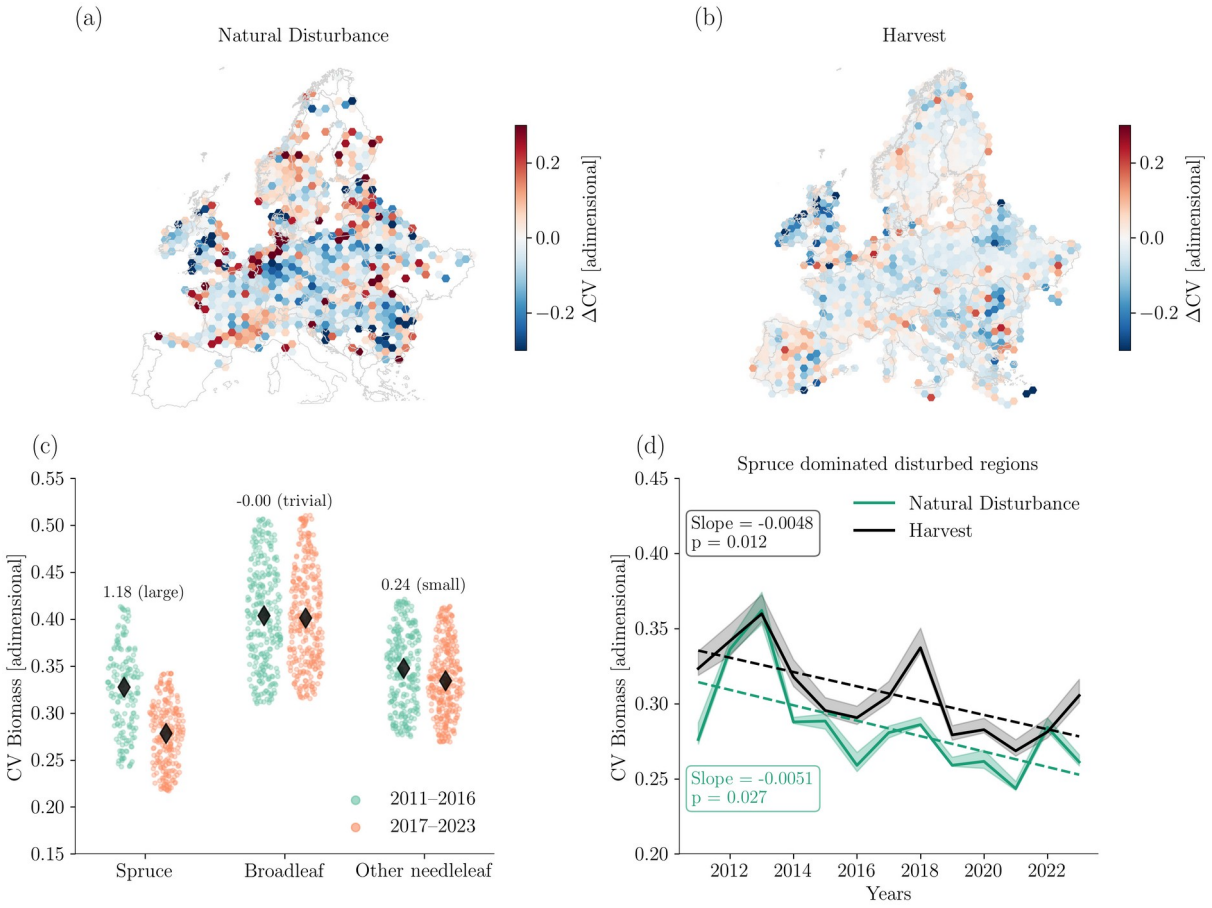

Figure 4: Changes in structural heterogeneity of disturbed forests across Europe. (a, b) Spatial changes in the coefficient of variation (CV) of aboveground biomass within disturbed pixels between 2011-2016 and 2017-2023, shown for (a) natural disturbances and (b) harvest. Biomass values reflect 2010 ESA CCI v6.0 estimates fixed prior to any disturbance within the study period. Blue shades indicate declining CV (more homogeneous forest patches), and red shades indicate increasing CV (more heterogeneous forest patches). (c) CV of biomass in disturbed pixels by genus group (spruce, broadleaf, other needleleaf) and period. Cohen's *d* effect sizes are reported above each comparison. (d) Temporal evolution of biomass CV in disturbed spruce-dominated pixels from 2011 to 2023, shown separately for natural disturbances and harvest. Lines represent the annual median CV across hexagons; shaded ribbons indicate the 5th to 95th percentile range across biomass members. Only 100 m pixels with at least 30% forest cover were retained, and among those, only pixels where at least 50% of the forested area was disturbed by a specific agent in a given year were considered. Each hexagon has a diameter of 100 km.

3.4 Amplifying biomass carbon susceptibility from natural disturbances.

If current disturbance patterns persist, natural disturbances alone could expose biomass carbon equivalent to approximately 20% of Europe's contemporary forest carbon sink (~210 TgC yr^{-1}) (Pan et al., 2024) by 2040. Under the recent biomass loss scenario, projected susceptibility reaches a median of ~48 TgC yr^{-1} (Fig. 5c), indicating that the carbon consequences of disturbance are intensifying beyond what would be expected from expanding disturbance area alone. This susceptibility represents carbon stocks transferred out of live forest biomass pools and rendered vulnerable to delayed recovery or longer-term loss, rather than immediate atmospheric fluxes. The projected susceptibility is geographically concentrated: Central European spruce forests, particularly the Bohemian Massif and surrounding mid-elevation ranges, emerge as primary hotspots under both scenarios (Fig. 5a). In contrast, harvest-related biomass carbon susceptibility, while larger in absolute magnitude (~143 TgC yr^{-1}), remains structurally stable and is concentrated mainly in Northern Europe (Fig. 5b).

Structural shifts toward older, higher-biomass, and more homogeneous landscapes substantially amplify future carbon susceptibility. Comparing the two scenarios isolates this effect: the early scenario uses the 2011-2016 biomass distribution of disturbed forest patches to forecast disturbance areas, whereas the recent scenario uses the 2017-2023 distribution. Under the recent scenario, natural disturbances are projected to expose a median of 47.6 TgC yr^{-1} (5th-95th percentile: 39.2-57.6), compared to 43.2 TgC yr^{-1} (35.5-52.6) under the early scenario, an increase of approximately 10% attributable primarily to the growing involvement of carbon-rich cohorts. Over the 2024-2040 projection period, this structural shift compounds to an additional ~75 TgC of biomass carbon susceptibility, equivalent to approximately one-third of Europe's contemporary annual forest carbon sink (210 TgC $year^{-1}$). By contrast, projected harvest-related biomass susceptibility remains structurally stable across scenarios (141.8 vs. 143.6 TgC yr^{-1}; ~1.3% change), indicating that harvest practices have not shifted toward systematically higher-biomass forest patches, as observed for natural disturbances.

This projected increasing carbon susceptibility results from the combined effects of expanding disturbance extent and increasing per-hectare biomass affected. Natural disturbances are projected to nearly double in spatial extent, from 0.38 Mha (0.19-0.75 Mha) in 2024 to 0.62 Mha (0.33-1.12 Mha) by 2040, whereas harvest expansion is more gradual (2.09 to 2.73 Mha; Fig. 5d). The steeper trajectory for natural disturbances reflects climate-sensititve amplification of bark beetle dynamics, while harvest areas remain aligned with management objectives and policy constraints. This interaction creates a multiplicative risk: even if future disturbance extent stabilises, continued targeting of carbon-rich forests would sustain elevated levels of biomass carbon susceptibility, thereby weakening the long-term effectiveness of Europe's forest carbon sink.

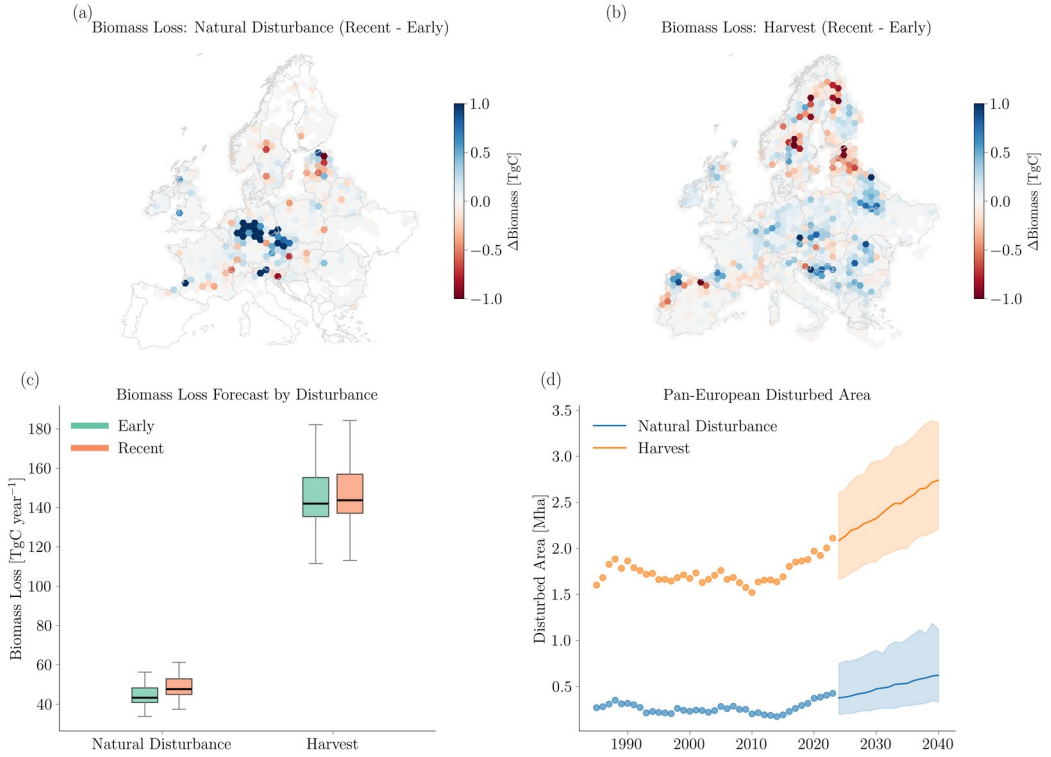

Figure 5: Forecasted biomass susceptibility and disturbed area across Europe through 2040 under early (2011-2016) and recent (2017-2023) disturbance scenarios. (a-b) Spatial differences in biomass susceptibility (PgC) between early and recent periods for natural disturbances (a) and harvest (b), with darker colours indicating larger increases in carbon susceptibility. (c) Boxplots of annual biomass susceptibility (TgC yr^{-1}) by disturbance type and scenario. Forecasts are based on smoothed trends (1985-2023), and model fits to the 2008-2023 window, assuming no change in forest management or spatial disturbance extent. Boxes represent the median and interquartile range across 20 biomass ensemble members; whiskers show the 5th and 95th percentiles. (d) Forecasted area of pan-European disturbed forests annually by natural disturbances and harvest. Points represent observed values (1985-2023); solid lines and shaded bands represent trend-based projections and their uncertainty ranges. Only 100 m pixels with at least 30% forest cover were retained, and among those, only pixels where at least 50% of the forested area was disturbed by a specific agent in a given year were considered. Hexagons with fewer than 50 valid pixels were excluded from analysis. Each hexagon has a diameter of 100 km.

Genus-specific projections show that spruce forests drive the amplification of biomass carbon susceptibility associated with natural disturbances (Fig. 6a). Under the recent scenario, spruce-dominated forests are projected to experience a median biomass carbon susceptibility of 21.4 TgC yr^{-1} (5th-95th percentile: 17.5-26.1), representing a 15% increase relative to the early scenario (18.6. TgC yr^{-1}; 15.1-22.8). In contrast, other needleleaf and broadleaf forests show only minor differences

between scenarios (12.3 vs. 11.5 TgC yr^{-1} and 11.1.3 vs. 10.5 TgC yr^{-1}, respectively), indicating that their disturbance-related carbon susceptibility scales primarily with expanding affected area rather than with shifts toward higher-biomass structural cohorts.

Harvest-related projections exhibit comparatively stable patterns across scenarios, with biomass carbon susceptibility dominated by other needleleaf (71.3 vs. 71.0 TgC yr^{-1}) and broadleaf forests (33.1 vs. 32.6 TgC yr^{-1}; Fig. 6b). Susceptibility associated with spruce harvests increases modestly (from 16.4 to 17.5 TgC yr^{-1}), likely reflecting enhanced salvage activity in beetle-affected regions rather than systematic shifts in harvest toward higher-biomass forest patches.

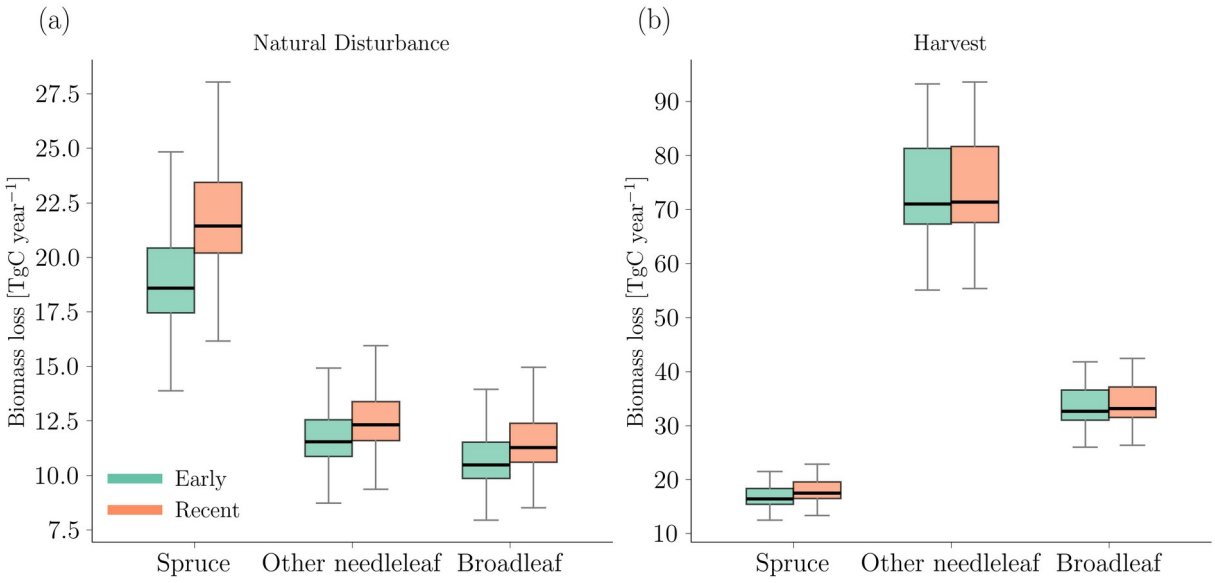

Figure 6: Forecasted biomass susceptibility across Europe through 2040 under early (2011-2016) and recent (2017-2023) disturbance scenarios and across dominant species. (a-b) Boxplots of annual biomass susceptibility (TgC yr^{-1}) for natural disturbances and harvest, stratified by scenario (early vs. recent) and by the dominant ~~species~~genus group of each hexagon. The dominant species was assigned as the genus ~~class~~group occupying the largest forested area within each 100-km hexagon. Forecasts are based on smoothed trends (1985-2023), and model fits to the 2008-2023 window, assuming no change in forest management or spatial disturbance extent. Boxes represent the median and interquartile range across 20 biomass ensemble members; whiskers show the 5th and 95th percentiles. Only 100 m pixels with at least 30% forest cover were retained, and among those, only pixels where at least 50% of the forested area was disturbed by a specific agent in a given year were considered. Hexagons with fewer than 50 valid pixels were excluded from analysis.

4 Discussion

Europe's forests face a compound susceptibility: climate-sensitive disturbances are increasingly concentrated in the continent's oldest, most carbon-dense landscapes, precisely those that underpin long-term carbon storage and took decades to develop. Our continental-scale analysis reveals that this structural selectivity occurs along three interacting dimensions: stand age, aboveground biomass, and structural homogeneity. Natural disturbances in forests >60 years old (2010 baseline age) nearly tripled between 2011-2016 and 2017-2023 (0.38 to 1.068 Mha), with impacts increasingly concentrated in forest patches exceeding 80 MgC ha^{-1} and exhibiting low biomass variation (CV decline: Cohen's d = 1.18 in spruce). This pattern represents not only an expansion of the extent of disturbance but also a qualitative shift in the forest structures most frequently affected, and therefore in the carbon stocks most exposed to rapid transfer from live-biomass pools. If these patterns persist, natural disturbances could expose biomass carbon equivalent to approximately 20% of Europe's contemporary forest carbon sink (~48 of ~210 TgC yr^{-1}) by 2040, with risks concentrated primarily in Central European spruce-dominated landscapes.

The observed shift in disturbance selectivity aligns spatially and temporally with climate-amplified bark beetle dynamics in spruce-dominated regions. Compound drought and heat events since 2018 have predisposed mature spruce stands to infestation, creating conditions for unprecedented intensification of outbreaks (Hermann et al., 2023; Weynants et al., 2024). Warming accelerates beetle development, enabling multiple generations per year and facilitating expansion into higher elevations and latitudes where historically cold temperatures had constrained outbreaks (Hartmann et al., 2025; Jakoby et al., 2019). While windstorms have historically caused episodic, large-scale forest losses (e.g., Lothar 1999, Klaus 2009), their spatially localised and temporally discrete nature does not align with the broad spatial coherence and multi-year persistence of the structural shift observed since 2017, a period during which bark beetles dominated disturbance activity across much of Central Europe (Patacca et al., 2023). The observed structural shift appears to be primarily driven by climate-amplified bark beetle outbreaks, rather than a systematic change in forest management. Harvest patterns remained structurally similar across periods, with only minor shifts in age and biomass distributions (median ED: 0.9 years). The strong spatial and temporal correspondence between the structural shift in natural disturbances and compound drought events since 2018 points to climate forcing as the primary driver. Nevertheless, longstanding management legacies, particularly decades of favouring monospecific spruce planting and increasing growing stocks, have maintained structural conditions that predispose these landscapes to continued outbreak amplification. It is worth noting that the majority of bark beetle-affected stands are subsequently salvage-logged, which explains the tight coupling between natural disturbance and harvest trajectories observed in our data (Pearson's r = 0.75). This coupling reflects a management response to disturbance rather than a driver of structural susceptibility, and is consistent with the structural stability we observe in harvest-related biomass distributions across periods.

Structural homogeneity is associated with increased susceptibility. Even-aged spruce monocultures provide continuous host connectivity, facilitating rapid beetle spread once outbreaks are initiated (Raffa et al., 2008). Such stands also lack vertical and horizontal structural complexity, reducing microclimatic buffering and increasing susceptibility to drought stress and heat accumulation, which further weakens host resistance (Senf and Seidl, 2018). Heterogeneous forests, by contrast, fragment host networks, maintain cooler and moister microclimates, and provide refugia for beetle predators and competitors (Seidl et al., 2016b).While structural and compositional diversity generally reduces susceptibility, long-term studies demonstrate that spruce decline can also occur in age- and species-diverse stands, suggesting that diversity increases but does not ensure resistance, and that site-level climate stress may outweigh the protective influence of structural diversity under prolonged drought conditions (Brzeziecki et al., 2020). While the mechanisms proposed here (i.e., host connectivity, microclimatic buffering, and predator refugia) operate at the forest-stand scale, our CV metric captures structural variability at the landscape scale (100 km hexagons). The declining CV we observe is therefore best interpreted as a landscape-level signal of increasing structural uniformity across the disturbance-active forest mosaic, which is consistent with, but not a direct measure of, the stand-level homogeneity that facilitates bark beetle spread.

Large-scale natural disturbances in Europe are frequently followed by salvage logging, which often leads to the re-establishment of extensive, even-aged spruce stands on affected sites (Sommerfeld et al., 2021). These post-disturbance management responses may contribute to maintaining, rather than disrupting, the structural conditions associated with high susceptibility, limiting the development of structural complexity that could otherwise enhance resistance. The near-identical temporal trajectories of CV decline in both naturally disturbed and harvested spruce forest patches (Pearson's $r = 0.84$) indicate a strong coupling between disturbance processes and management responses, suggesting that harvest activity increasingly mirrors disturbance patterns rather than proactively reducing long-term susceptibility. This coupling is most pronounced in Central Europe, where decades of homogeneous spruce planting have produced landscapes highly prone to outbreak amplification under climate stress.

Outbreak dynamics further reinforce this structural susceptibility. Early in disturbance cycles, infestations often target physiologically weakened hosts; however, during outbreak peaks, such as those following the 2018 drought, high beetle populations can overwhelm even relatively vigorous trees, diminishing the role of individual tree resistance and further concentrating impacts in structurally uniform landscapes (Senf and Seidl, 2021). Together, these outbreak dynamics and the post-disturbance management responses described above help explain why spruce-dominated regions exhibit the most substantial and most persistent declines in structural heterogeneity, and why homogeneous forest patches continue to incur disproportionate disturbance impacts even as climate stress expands susceptibility to younger pine and spruce plantations in parts of Eastern Europe (Davydenko et al., 2021; Siitonen, 2014).

The three dimensions of structural selectivity we document (i.e, age, biomass, and homogeneity) are closely linked rather than independent. Biomass accumulation occurs across multiple forest types, including naturally developing beech-

dominated forests in Europe (Schütz, 2002). In the context of our study, however, biomass accumulation most strongly amplifies disturbance susceptibility in even-aged spruce monocultures, where it combines with structural homogeneity and elevated drought sensitivity. Central European spruce monocultures frequently combine advanced 2010 baseline age (>60 years), high 2010 baseline carbon density (>80 MgC ha^{-1}), and low structural diversity. Our results indicate that forests combining these characteristics exhibit disproportionately high susceptibility. Such forest patches dominate the Bohemian Massif and surrounding mid-elevation ranges of Austria, Germany, and the Czech Republic, consistent with the geographic concentration of disturbance-related carbon susceptibility identified in our spatial projections (Fig. 5a).

This convergence of vulnerabilities explains why a relatively small fraction of Europe's forest area contributes disproportionately to disturbance-related carbon susceptibility. Spruce forests accounted for roughly 44% of the naturally disturbed area in the recent period, yet contributed approximately 52% of disturbance-associated biomass carbon losses, with a more than fivefold increase between periods (11.5 to 62.3 TgC). This is consistent with independent evidence that the sensitivity of biomass loss to disturbed area increased in European temperate forests after 2018 (Kowalski et al., 2026), indicating that disturbance area alone is an increasingly poor predictor of carbon consequences. Our results identify the structural basis for that decoupling: a shift toward older, higher-biomass, and more homogeneous spruce cohorts. Regional contrasts further support this interpretation: Western and Central Europe experienced pronounced shifts toward older impacted cohorts beginning around 2017, coinciding with prolonged compound drought conditions through 2022. In contrast, parts of Eastern and Southeastern Europe showed relatively greater impacts in younger (approximately 40-50 years old) pine and spruce plantations, which often exhibit high stem densities, limited thinning, and elevated drought sensitivity (Jaime et al., 2022).

The compound nature of this susceptibility implies that effective climate adaptation cannot rely on single-axis interventions. Age diversification alone may not protect structurally homogeneous spruce forest patches from drought-amplified beetle outbreaks; species diversification without increased structural complexity may merely shift the vulnerable cohort; and structural thinning in climatically marginal regions may, in some cases, exacerbate drought stress. Reducing future susceptibility will likely require coordinated management of species composition, structural complexity, and spatial heterogeneity.

These findings have direct implications for proposed strategies to enhance forest carbon storage. For instance, our results raise an important caveat regarding proforestation, the strategy of withdrawing managed stands from harvest and allowing them to age naturally to accumulate carbon. While proforestation can substantially increase carbon stocks in the medium term (Moomaw et al., 2019), our findings reveal a structural susceptibility that can partially counteract its expected carbon benefits: the structural characteristics that proforestation promotes, namely advanced age and greater biomass accumulation overtime, are precisely those now associated with disproportionate disturbance susceptibility in Central Europe's spruce-dominated forests. This does not, however, invalidate proforestation as a strategy for increasing forest carbon storage. In

broadleaf and structurally diverse ecosystems, for instance, the susceptibility we document is substantially lower. However, our findings underscore that the effectiveness of proforestation strategies is strongly species- and region-dependent. In spruce-dominated landscapes, proforestation without concurrent efforts to increase structural and compositional diversity may not fully realise its expected carbon benefits, given the elevated disturbance susceptibility of ageing, high-biomass stands documented here. Conversely, in broadleaf-dominated or structurally complex systems with lower susceptibility to disturbance, proforestation remains a promising complement to active management strategies.

Our projection that natural disturbances could expose biomass carbon equivalent to approximately 20% of Europe's forest carbon sink by 2040 is conservative by design. We assume no further geographic expansion of bark beetle outbreaks beyond current ranges, despite documented upward and northward spread (Hartmann et al., 2025, Junttila et al., 2024; Kärvemo et al., 2023) and model-based projections of intensifying disturbance pressure under continued warming (Grünig et al., 2026). We also exclude post-disturbance mortality cascades and assume historical recovery rates, even though recurrent disturbances increasingly slow regrowth and may induce persistent ecosystem state shifts (Forzieri et al., 2022; Senf and Seidl, 2022). Management practices are held constant, although future changes in harvesting, salvage strategies, or species composition could substantially alter disturbance susceptibility.

Beyond these structural assumptions, the analysis rests on observational datasets that carry their own sources of uncertainty. The European Forest Disturbance Atlas primarily detects stand-replacing canopy loss events and may miss gradual or partial disturbances, such as progressive drought-induced dieback or low-severity insect damage. Our analysis, therefore, captures the most severe end of the disturbance spectrum, and patterns in lower-severity events may differ. The GAMIv3.0 age product carries inherent uncertainty, particularly in forests with complex management histories, which could propagate into the energy distance calculations and age-class comparisons. We address this by propagating uncertainty across the full 20-member age ensemble and reporting 5th-95th percentile ranges throughout. ESA CCI biomass data carry inherent limitations in the calibration of aboveground carbon estimates from remote sensing observations, as the sensitivity of satellite-derived retrievals decreases with increasing biomass, contributing to uncertainty that is disproportionately large in high-biomass forests (Santoro et al., 2024). Biomass uncertainty is explicitly propagated through 20 independent realisations of the ESA CCI v6.0 product, by introducing controlled perturbations to the mean estimates, scaled by the per-pixel standard deviation, ensuring that uncertainty is largest where retrieval uncertainty is greatest. All biomass-dependent results are reported as ensemble medians with 5th-95th percentile ranges. The 50-pixel hexagon retention threshold may also introduce a geographic bias toward regions with elevated disturbance activity, as landscape units with sparse disturbance records are excluded from the analysis. This means that the continental estimates reported here may overrepresent structurally vulnerable, high-disturbance landscapes and may not fully reflect conditions in low-disturbance regions. Readers should therefore interpret the pan-European summaries as characterising the most dynamically active portions of the European forest domain rather than the full breadth of European forest conditions.

The persistence of the background landscape biomass distribution across periods (Fig. S7) confirms that the observed shift toward higher-biomass disturbed forest patches reflects an actual change in disturbance selectivity rather than a consequence of either biomass accumulation or the progressive loss of lower-biomass forest patches through the 2011-2016 disturbance activity. Each of these excluded processes and data limitations would tend to amplify rather than dampen projected carbon susceptibility. Forecast uncertainty remains substantial, with 5th-95th percentile ranges spanning approximately ±20% around median estimates (Fig. 5c), reflecting interannual variability in disturbance activity (captured via Taylor's law variance scaling; Taylor, 1961), uncertainty in biomass estimates, and stochastic extremes such as storm events or outbreak collapses (Senf et al., 2025). Notably, even the lower bounds of projected natural-disturbance-related biomass susceptibility (35.5-39.2 TgC yr^{-1}) exceed upper estimates from the early 2010s (~13.9 TgC yr^{-1}; Section 3.2), indicating that intensification is robust across plausible trajectories. Accordingly, the estimated 20% sink offset should be interpreted as a near-term baseline risk rather than a worst-case outcome.

5 Conclusion

Our findings reveal a clear divergence in contemporary disturbance dynamics across Europe's forests. Natural disturbances increasingly affect older, carbon-dense spruce landscapes in Central Europe. In contrast, harvest activities remain structurally stable and are more frequently concentrated in younger or lower-biomass forests. This divergence reflects a growing structural selectivity of climate-sensitive natural disturbances, particularly bark beetle outbreaks, which now disproportionately expose carbon-rich and structurally mature forest cohorts. As a result, disturbance impacts are not only expanding in area but are increasingly concentrated in forest structures that store large amounts of biomass accumulated over decades.

The concentration of disturbance impacts in these vulnerable cohorts implies that Europe's disturbance-related carbon susceptibility is likely to intensify and spatially consolidate in regions dominated by mature spruce forests. Because recovery rates in older, high-biomass forest patches are typically slower and marginal carbon uptake is lower than in younger forests, disturbances affecting these cohorts have disproportionate implications for long-term forest carbon storage, even when regrowth ultimately occurs. Consequently, moderate increases in disturbance frequency or extent can translate into amplified, continent-scale reductions in the effectiveness of the forest carbon sink.

If current trajectories persist, natural disturbances alone could expose a substantial share of Europe's land-based forest carbon sequestration capacity over the coming decades. Addressing this emerging risk requires re-evaluating the drivers of forest structural susceptibility and implementing adaptive management strategies that enhance resilience to climate-sensitive disturbances. Several measures like increasing species and structural diversity have been proposed to reduce susceptibility in high-risk stands. Targeted interventions promote mixed-species composition, structural thinning reduces stem density and host connectivity, while adopting uneven-aged management in climatically marginal spruce-dominated landscapes and

refining harvest and post-disturbance management practices in disturbance-prone regions will further reduce susceptibility (Migliavacca et al., 2025). The effectiveness of such strategies will depend on their ability to reduce structural homogeneity and interrupt feedback between disturbance processes and management responses.

Improved monitoring of disturbance and mortality remains crucial for predicting carbon losses and informing policy. This includes coordinated, EU-wide data collection (Network, 2025; Zweifel et al., 2023) and collaborative platforms, such as *deadtrees.earth* (Mosig et al., 2024). Integrating national assessments into open-access systems would strengthen both scientific modelling and policy implementation under frameworks such as the EU Forest Strategy for 2030 ("Communication," n.d.), the LULUCF Regulation (Regulation (EU) 2023/839) ("Regulation - 2023/839 - EN - EUR-Lex," n.d.), and the Nature Restoration Regulation (Regulation (EU) 2024/1991) ("Regulation - EU - 2024/1991 - EN - EUR-Lex," n.d.). As Europe advances these ambitious forest policies, explicitly recognising and mitigating the growing susceptibility of its oldest and most carbon-rich forests will be critical for safeguarding the continent's land carbon sink in a warming climate.

Data availability.

- The European Forest Disturbance Atlas v2.1.1 is available from Viana-Soto and Senf (2025) at https://doi.org/10.5194/essd-17-2373-2025.
- Forest age data (Global Age Mapping Integration v3.0) are available from Besnard et al. (2023) at https://doi.org/10.5880/GFZ.1.4.2023.006.
- Aboveground biomass data (ESA CCI Biomass v6.0) are available from Santoro and Cartus (2025) at https://catalogue.ceda.ac.uk/uuid/95913ffb6467447ca72c4e9d8cf30501/.
- European forest genus classification data are available from De Keersmaecker et al. (2024) at https://doi.org/10.5281/zenodo.13341104.

All processed datasets underlying the analyses and figures presented in this study are publicly available via Zenodo at: **https://doi.org/10.5281/zenodo.17977435**. The Zenodo repository contains aggregated disturbance metrics, forest age and biomass distributions, structural heterogeneity metrics, and projection outputs used to generate the figures. All files are provided in open formats.

Code availability.

All code for data integration, statistical analysis, forecasting, and visualisation is available at https://github.com/simonbesnard1/structshift. The repository includes Python scripts for disturbance-demographic integration, Energy Distance calculations, ensemble forecasting, and figure generation. Documentation and example workflows are provided in the repository README.

Authors contributions

SB designed the research, performed the analysis, and drafted the manuscript. The study builds on an original idea developed by CS. SB also prepared the GAMIv3.0 dataset. AVS and CS prepared the European Forest Disturbance Atlas maps; WDK and RVDK provided the genus distribution maps; and MS prepared the ESA-CCI biomass product. All authors contributed to the interpretation of results and provided critical feedback on the manuscript. This work is the outcome of a research exchange of SB and VH to TU München.

Competing interests.

The authors declare that they have no conflict of interest.

Acknowledgements

We thank the Global Land Monitoring group members at the GFZ Helmholtz Centre for Geosciences for providing feedback on the presented results. We thank the GFZ Helmholtz Centre for Geosciences for providing the computational and data infrastructure that enabled this research. We recognise the use of OpenAI's ChatGPT and Grammarly AI tools to assist with improving sentence structure, clarity, and grammar during manuscript preparation. Importantly, we emphasise that all research design, data analysis, interpretation of results, and conclusions presented in this study are entirely our own.

Financial support

SB and VH acknowledge funding support by the European Union through the FORWARDS (https://forwards-project.eu/), OpenEarthMonitor (https://earthmonitor.org/), and NextGenCarbon (https://www.nextgencarbon-project.eu/) projects. AVS, CS, WDK, and RVDK acknowledge funding from the ForestPaths project (https://forestpaths.eu/). AVS and CS further acknowledge funding from the European Space Agency (CLIMATE SPACE RECCAP2; 4000144908/24/I-LR) and the Federal Ministry of Education and Research (BMBF) (AI4Forest; 01IS23025C).

References

Bergkvist, J., Lagergren, F., Islam, Md.R., Wårlind, D., Miller, P.A., Finnander Linderson, M.-L., Lindeskog, M., Jönsson, A.M., 2025. Quantifying the Impact of Climate Change and Forest Management on Swedish Forest Ecosystems Using the Dynamic Vegetation Model LPJ-GUESS. Earth's Future 13, e2024EF004662. https://doi.org/10.1029/2024EF004662

Berthelot, S., Frühbrodt, T., Hajek, P., Nock, C.A., Dormann, C.F., Bauhus, J., Fründ, J., 2021. Tree diversity reduces the risk of bark beetle infestation for preferred conifer species, but increases the risk for less preferred hosts. J. Ecol. 109, 2649–2661. https://doi.org/10.1111/1365-2745.13672

Besnard, S., Heinrich, V.H.A., Carvalhais, N., Ciais, P., Herold, M., Luijkx, I., Peters, W., Requena Suarez, D., Santoro, M., Yang, H., 2025. Global covariation of forest age transitions with the net carbon balance. Nat. Ecol. Evol. 1–13. https://doi.org/10.1038/s41559-025-02821-5

Besnard, S., Koirala, S., Santoro, M., Weber, U., Nelson, J., Gütter, J., Herault, B., Kassi, J., N'Guessan, A., Neigh, C., Poulter, B., Zhang, T., Carvalhais, N., 2021. Mapping global forest age from forest inventories, biomass and climate data. Earth Syst. Sci. Data 13, 4881–4896. https://doi.org/10.5194/essd-13-4881-2021

Besnard, S., Santoro, M., Herold, M., Cartus, Oliver, Gütter, J., Heinrich, V.H.A., Herault, B., Kassi, J., Koirala, S., N'Guessan, A., Neigh, C., Nelson, J.A., Poulter, B., Weber, U., Zhang, T., Carvalhais, N., n.d. Global Age Mapping Integration (GAMI). V. 2.0. https://doi.org/10.5880/GFZ.1.4.2023.006

Brockerhoff, E.G., Jactel, H., Parrotta, J.A., Quine, C.P., Sayer, J., 2008. Plantation forests and biodiversity: oxymoron or opportunity? Biodivers. Conserv. 17, 925–951. https://doi.org/10.1007/s10531-008-9380-x

Brzeziecki, B., Woods, K., Bolibok, L., Zajączkowski, J., Drozdowski, S., Bielak, K., Żybura, H., 2020. Over 80 years without major disturbance, late-successional Białowieża woodlands exhibit complex dynamism, with coherent compositional shifts towards true old-growth conditions. J. Ecol. 108, 1138–1154. https://doi.org/10.1111/1365-2745.13367

Calle, L., Poulter, B., 2021. Ecosystem age-class dynamics and distribution in the LPJ-wsl v2.0 global ecosystem model. Geosci. Model Dev. 14, 2575–2601. https://doi.org/10.5194/gmd-14-2575-2021

Ceccherini, G., Duveiller, G., Grassi, G., Lemoine, G., Avitabile, V., Pilli, R., Cescatti, A., 2020. Abrupt increase in harvested forest area over Europe after 2015. Nature 583, 72–77. https://doi.org/10.1038/s41586-020-2438-y

Communication: New EU Forest Strategy for 2030 | European Commission [WWW Document], n.d. URL https://commission.europa.eu/document/cf3294e1-8358-4c93-8de4-3e1503b95201_en (accessed 7.30.25).

Davydenko, K., Vasaitis, R., Elfstrand, M., Baturkin, D., Meshkova, V., Menkis, A., 2021. Fungal Communities Vectored by Ips sexdentatus in Declining Pinus sylvestris in Ukraine: Focus on Occurrence and Pathogenicity of Ophiostomatoid Species. Insects 12, 1119. https://doi.org/10.3390/insects12121119

De Keersmaecker, W., Zanaga, D., Viana-Soto, A., Senf, C., Van De Kerchove, R., 2024. ForestPaths: European genus map.

Forzieri, G., Dakos, V., McDowell, N.G., Ramdane, A., Cescatti, A., 2022. Emerging signals of declining forest resilience under climate change. Nature 608, 534–539. https://doi.org/10.1038/s41586-022-04959-9

Grünig, M., Rammer, W., Senf, C., Albrich, K., André, F., Augustynczik, A.L.D., Baumann, M., Bohn, F.J., Bouwman, M., Bugmann, H., Collalti, A., Cristal, I., Dalmonech, D., De Coligny, F., Dobor, L., Dollinger, C., Espelta, J.M., Forrester, D.I., Garcia-Gonzalo, J., González-Olabarria, J.R., Hiltner, U., Hlásny, T., Honkaniemi, J., Huber, N., Jonard, M., Jönsson, A.M., Kunstler, G., Lagergren, F., Lindner, M., Mina, M., Moos, C., Morin, X., Muys, B., Nabuurs, G.-J., Nieberg, M., Patacca, M., Peltoniemi, M., Reyer, C.P.O., Schelhaas, M.-J., Storms, I., Thom, D., Toïgo, M., Seidl, R., 2026. Climate change will increase forest disturbances in Europe throughout the 21st century. Science 391, eadx6329. https://doi.org/10.1126/science.adx6329

Hansen, M.C., Potapov, P.V., Moore, R., Hancher, M., Turubanova, S.A., Tyukavina, A., Thau, D., Stehman, S.V., Goetz, S.J., Loveland, T.R., Kommareddy, A., Egorov, A., Chini, L., Justice, C.O., Townshend, J.R.G., 2013. High-Resolution Global Maps of 21st-Century Forest Cover Change. Science 342, 850–853. https://doi.org/10.1126/science.1244693

Hartmann, H., Battisti, A., Brockerhoff, E., Bełka, M., Hurling, R., Jactel, H., Oliva, J., Rousselet, J., Terhonen, E., Ylioja, T., Melin, M., Olson, Å., De Prins, F., Zhang, K., Stein Åslund, M., Davydenko, K., Menkis, A., Elfstrand, M., Zúbrik, M., Kunca, A., Galko, J., Paulin, M., Csóka, G., Hoch, G., Pernek, M., Preidl, S., Fischer, R., 2025. European forests are under increasing pressure from global change-driven invasions and accelerating epidemics by insects and diseases. Themenh. Waldschutz Im Klimawandel 77, 6–24. https://doi.org/10.5073/JfK.2025.02.02

Hermann, M., Röthlisberger, M., Gessler, A., Rigling, A., Senf, C., Wohlgemuth, T., Wernli, H., 2023. Meteorological history of low-forest-greenness events in Europe in 2002–2022. Biogeosciences 20, 1155–1180. https://doi.org/10.5194/bg-20-1155-2023

Hlásny, T., König, L., Krokene, P., Lindner, M., Montagné-Huck, C., Müller, J., Qin, H., Raffa, K.F., Schelhaas, M.-J., Svoboda, M., Viiri, H., Seidl, R., 2021. Bark Beetle Outbreaks in Europe: State of Knowledge and Ways Forward for Management. Curr. For. Rep. 7, 138–165. https://doi.org/10.1007/s40725-021-00142-x

International Tree Mortality Network, 2025. Towards a global understanding of tree mortality. New Phytol. 245, 2377–2392. https://doi.org/10.1111/nph.20407

Jaime, L., Batllori, E., Ferretti, M., Lloret, F., 2022. Climatic and stand drivers of forest resistance to recent bark beetle disturbance in European coniferous forests. Glob. Change Biol. 28, 2830–2841. https://doi.org/10.1111/gcb.16106

Jakoby, O., Lischke, H., Wermelinger, B., 2019. Climate change alters elevational phenology patterns of the European spruce bark beetle (Ips typographus). Glob. Change Biol. 25, 4048–4063. https://doi.org/10.1111/gcb.14766

Junttila, S., Blomqvist, M., Laukkanen, V., Heinaro, E., Polvivaara, A., O'Sullivan, H., Yrttimaa, T., Vastaranta, M., Peltola, H., 2024. Significant increase in forest canopy mortality in boreal forests in Southeast Finland. For. Ecol. Manag. 565, 122020. https://doi.org/10.1016/j.foreco.2024.122020

Kärvemo, S., Huo, L., Öhrn, P., Lindberg, E., Persson, H.J., 2023. Different triggers, different stories: Bark-beetle infestation patterns after storm and drought-induced outbreaks. For. Ecol. Manag. 545, 121255. https://doi.org/10.1016/j.foreco.2023.121255

Korhonen K. T., Ahola A. et al. (2021) Forests of Finland 2014–2018 and their development 1921–2018 [WWW Document], n.d. URL https://www.silvafennica.fi/article/10662 (accessed 7.3.25).

Kowalski, K., Viana-Soto, A., Brandt, M., Ciais, P., De Keersmaecker, W., Fensholt, R., Pugh, T.A.M., Xu, Y., Senf, C., 2026. Accelerating biomass loss from forest disturbances across Europe. Nat. Geosci. https://doi.org/10.1038/s41561-026-02032-y

Lindegaard, K.N., Adams, P.W.R., Holley, M., Lamley, A., Henriksson, A., Larsson, S., Lopez, G.E., Pisarek, M., 2016. Short rotation plantations policy history in Europe: Lessons from the past and recommendations for the future. Food Energy Secur. 5, 125–152. https://doi.org/10.1002/fes3.86

Living with bark beetles: impacts, outlook and management options | European Forest Institute [WWW Document], 2019. URL https://efi.int/publications-bank/living-bark-beetles-impacts-outlook-and-management-options (accessed 7.8.25).

Migliavacca, M., Grassi, G., Bastos, A., Ceccherini, G., Ciais, P., Janssens-Maenhout, G., Lugato, E., Mahecha, M.D., Novick, K.A., Peñuelas, J., Pilli, R., Reichstein, M., Avitabile, V., Beck, P.S.A., Barredo, J.I., Forzieri, G., Herold, M., Korosuo, A., Mansuy, N., Mubareka, S., Orth, R., Rougieux, P., Cescatti, A., 2025. Securing the forest carbon sink for the European Union's climate ambition. Nature 643, 1203–1213. https://doi.org/10.1038/s41586-025-08967-3

Moomaw, W.R., Masino, S.A., Faison, E.K., 2019. Intact forests in the United States: Proforestation mitigates climate change and serves the greatest good. Front. For. Glob. Change 2, 27. https://doi.org/10.3389/ffgc.2019.00027

Mosig, C., Vajna-Jehle, J., Mahecha, M.D., Cheng, Y., Hartmann, H., Montero, D., Junttila, S., Horion, S., Schwenke, M.B., Adu-Bredu, S., Al-Halbouni, D., Allen, M., Altman, J., Angiolini, C., Astrup, R., Barrasso, C., Bartholomeus, H., Brede, B., Buras, A., Carrieri, E., Chirici, G., Cloutier, M., Cushman, K.C., Dalling, J.W., Dempewolf, J., Denter, M., Ecke, S., Eichel, J., Eltner, A., Fabi, M., Fassnacht, F., Feirreira, M.P., Frey, J., Frick, A., Ganz, S., Garbarino, M., García, M., Gassilloud, M., Ghasemi, M., Giannetti, F., Gonzalez, R., Gosper, C., Greinwald, K., Grieve, S., Gutierrez, J.A., Göritz, A., Hajek, P., Hedding, D., Hempel, J., Hernández, M., Heurich, M., Honkavaara, E., Jucker, T., Kalwij, J.M., Khatri-Chhetri, P., Klemmt, H.-J., Koivumäki, N., Korznikov, K., Kruse, S., Krüger, R., Laliberté, E., Langan, L., Latifi, H., Lehmann, J., Li, L., Lines, E., Lopatin, J., Lucieer, A.,

Ludwig, M., Ludwig, A., Lyytikäinen-Saarenmaa, P., Ma, Q., Marino, G., Maroschek, M., Meloni, F., Menzel, A., Meyer, H., Miraki, M., Moreno-Fernández, D., Muller-Landau, H.C., Mälicke, M., Möhring, J., Müllerova, J., Neumeier, P., Näsi, R., Oppgenoorth, L., Palmer, M., Paul, T., Potts, A., Prober, S., Puliti, S., Pérez-Priego, O., Reudenbach, C., Rossi, C., Ruehr, N.K., Ruiz-Benito, P., Runge, C.M., Scherer-Lorenzen, M., Schiefer, F., Schladebach, J., Schmehl, M.-T., Schwarz, S., Seidl, R., Shafeian, E., Simone, L. de, Sohrabi, H., Sotomayor, L., Sparrow, B., Steer, B.S.C., Stenson, M., Stöckigt, B., Su, Y., Suomalainen, J., Torresani, M., Umlauft, J., Vargas-Ramírez, N., Volpi, M., Vásquez, V., Weinstein, B., Ximena, T.C., Zdunic, K., Zielewska-Büttner, K., Oliveira, R.A. de, Wagtendonk, L. van, Dosky, V. von, Kattenborn, T., 2024. deadtrees.earth - An Open-Access and Interactive Database for Centimeter-Scale Aerial Imagery to Uncover Global Tree Mortality Dynamics. https://doi.org/10.1101/2024.10.18.619094

Nabuurs, G.-J., Lindner, M., Verkerk, P.J., Gunia, K., Deda, P., Michalak, R., Grassi, G., 2013. First signs of carbon sink saturation in European forest biomass. Nat. Clim. Change 3, 792–796. https://doi.org/10.1038/nclimate1853

Neuner, S., Albrecht, A., Cullmann, D., Engels, F., Griess, V.C., Hahn, W.A., Hanewinkel, M., Härtl, F., Kölling, C., Staupendahl, K., Knoke, T., 2015. Survival of Norway spruce remains higher in mixed stands under a dryer and warmer climate. Glob. Change Biol. 21, 935–946. https://doi.org/10.1111/gcb.12751

O'Sullivan, M., Sitch, S., Friedlingstein, P., Luijkx, I.T., Peters, W., Rosan, T.M., Arneth, A., Arora, V.K., Chandra, N., Chevallier, F., Ciais, P., Falk, S., Feng, L., Gasser, T., Houghton, R.A., Jain, A.K., Kato, E., Kennedy, D., Knauer, J., McGrath, M.J., Niwa, Y., Palmer, P.I., Patra, P.K., Pongratz, J., Poulter, B., Rödenbeck, C., Schwingshackl, C., Sun, Q., Tian, H., Walker, A.P., Yang, D., Yuan, W., Yue, X., Zaehle, S., 2024. The key role of forest disturbance in reconciling estimates of the northern carbon sink. Commun. Earth Environ. 5, 1–10. https://doi.org/10.1038/s43247-024-01827-4

Pan, Y., Birdsey, R.A., Phillips, O.L., Houghton, R.A., Fang, J., Kauppi, P.E., Keith, H., Kurz, W.A., Ito, A., Lewis, S.L., Nabuurs, G.-J., Shvidenko, A., Hashimoto, S., Lerink, B., Schepaschenko, D., Castanho, A., Murdiyarso, D., 2024. The enduring world forest carbon sink. Nature 631, 563–569. https://doi.org/10.1038/s41586-024-07602-x

Patacca, M., Lindner, M., Lucas-Borja, M.E., Cordonnier, T., Fidej, G., Gardiner, B., Hauf, Y., Jasinevičius, G., Labonne, S., Linkevičius, E., Mahnken, M., Milanovic, S., Nabuurs, G.-J., Nagel, T.A., Nikinmaa, L., Panyatov, M., Bercak, R., Seidl, R., Ostrogović Sever, M.Z., Socha, J., Thom, D., Vuletic, D., Zudin, S., Schelhaas, M.-J., 2023. Significant increase in natural disturbance impacts on European forests since 1950. Glob. Change Biol. 29, 1359–1376. https://doi.org/10.1111/gcb.16531

Pulgarin Diaz J. A., Melin M. et al. (2024) Relationship between stand and landscape attributes and *Ips typographus* salvage loggings in Finland [WWW Document], n.d. URL https://www.silvafennica.fi/article/23069 (accessed 7.3.25).

Raffa, K.F., Aukema, B.H., Bentz, B.J., Carroll, A.L., Hicke, J.A., Turner, M.G., Romme, W.H., 2008. Cross-scale Drivers of Natural Disturbances Prone to Anthropogenic Amplification: The Dynamics of Bark Beetle Eruptions. BioScience 58, 501–517. https://doi.org/10.1641/B580607

Regulation - 2023/839 - EN - EUR-Lex [WWW Document], n.d. URL https://eur-lex.europa.eu/eli/reg/2023/839/oj/eng (accessed 7.8.25).

Regulation - EU - 2024/1991 - EN - EUR-Lex [WWW Document], n.d. URL https://eur-lex.europa.eu/legal-content/EN/TXT/?uri=CELEX%3A32024R1991&qid=1722240349976 (accessed 7.28.25).

Ritter, F., Ciais, P., Senf, C., Santoro, M., Xu, Y., Pelissier-Tanon, A., Schwartz, M., Fayad, I., Carvalhais, N., Brandt, M., Fensholt, R., Besnard, S., Avitabile, V., 2025. Alarming decline in the carbon sink of European forests driven by disturbances. https://doi.org/10.21203/rs.3.rs-3671432/v1

Rizzo, M.L., Székely, G.J., 2016. Energy distance. WIREs Comput. Stat. 8, 27–38. https://doi.org/10.1002/wics.1375

Santoro, M., Cartus, O., Quegan, S., Kay, H., Lucas, R.M., Araza, A., Herold, M., Labrière, N., Chave, J., Rosenqvist, Å. and Tadono, T., 2024. Design and performance of the Climate Change Initiative Biomass global retrieval algorithm. Science of remote sensing, 10, p.100169.

Santoro, M., Cartus, O., 2025. ESA Biomass Climate Change Initiative (Biomass_cci): Global datasets of forest above-ground biomass for the years 2007, 2010, 2015, 2016, 2017, 2018, 2019, 2020, 2021 and 2022, v6.0. NERC EDS Centre for Environmental Data Analysis. https://doi.org/10.5285/95913ffb6467447ca72c4e9d8cf30501

Schelhaas, M.J., Nabuurs, G.J., Schuck, A., 2003. Natural disturbances in the European forests in the 19th and 20th centuries. Glob. Change Biol. 9, 1620–1633. https://doi.org/10.1046/j.1365-2486.2003.00684.x

Schütz, J.P., 2002. Silvicultural tools to develop irregular and diverse forest structures. Forestry 75, 329–337. https://doi.org/10.1093/forestry/75.4.329

Seidl, R., Schelhaas, M.J., Rammer, W., Verkerk, P.J., 2014. Increasing forest disturbances in Europe and their impact on carbon storage. Nat. Clim. Change 4, 806–810. https://doi.org/10.1038/nclimate2318

Seidl, R., Müller, J., Hothorn, T., Bässler, C., Heurich, M., Kautz, M., 2016a. Small beetle, large-scale drivers: how regional and landscape factors affect outbreaks of the European spruce bark beetle. J. Appl. Ecol. 53, 530–540. https://doi.org/10.1111/1365-2664.12540

Seidl, R., Donato, D.C., Raffa, K.F., Turner, M.G., 2016b. Spatial variability in tree regeneration after wildfire delays and dampens future bark beetle outbreaks. Proc. Natl. Acad. Sci. 113, 13075–13080. https://doi.org/10.1073/pnas.1615263113

Seidl, R., Senf, C., 2024. Changes in planned and unplanned canopy openings are linked in Europe's forests. Nat. Commun. 15, 4741. https://doi.org/10.1038/s41467-024-49116-0

Senf, C., Seidl, R., 2022. Post-disturbance canopy recovery and the resilience of Europe's forests. Glob. Ecol. Biogeogr. 31, 25–36. https://doi.org/10.1111/geb.13406

Senf, C., Seidl, R., 2021. Persistent impacts of the 2018 drought on forest disturbance regimes in Europe. Biogeosciences 18, 5223–5230. https://doi.org/10.5194/bg-18-5223-2021

Senf, C., Seidl, R., 2018. Natural disturbances are spatially diverse but temporally synchronized across temperate forest landscapes in Europe. Glob. Change Biol. 24, 1201–1211. https://doi.org/10.1111/gcb.13897

Senf, C., Seidl, R., Knoke, T., Jucker, T., 2025. Taylor's law predicts unprecedented pulses of forest disturbance under global change. Nat. Commun. 16, 6133. https://doi.org/10.1038/s41467-025-61585-5

Siitonen, J., 2014. *Ips acuminatus* kills pines in southern Finland. Silva Fenn. 48.

Sommerfeld, A., Rammer, W., Heurich, M., Hilmers, T., Müller, J., Seidl, R., 2021. Do bark beetle outbreaks amplify or dampen future bark beetle disturbances in Central Europe? J. Ecol. 109, 737–749. https://doi.org/10.1111/1365-2745.13502

Suvanto, S., Esquivel-Muelbert, A., Schelhaas, M.J., Astigarraga, J., Astrup, R., Cienciala, E., Fridman, J., Henttonen, H.M., Kunstler, G., Kändler, G., König, L.A., Ruiz-Benito, P., Senf, C., Stadelmann, G., Starcevic, A., Talarczyk, A., Zavala, M.A., Pugh, T.A.M., 2025. Understanding Europe's forest harvesting regimes. Earth's Future 13, e2024EF005225. https://doi.org/10.1029/2024EF005225

Taylor, L.R., 1961. Aggregation, Variance and the Mean. Nature 189, 732–735. https://doi.org/10.1038/189732a0

Turubanova, S., Potapov, P., Hansen, M.C., Li, X., Tyukavina, A., Pickens, A.H., Hernandez-Serna, A., Arranz, A.P., Guerra-Hernandez, J., Senf, C., Häme, T., Valbuena, R., Eklundh, L., Brovkina, O., Navrátilová, B., Novotný,

J., Harris, N., Stolle, F., 2023. Tree canopy extent and height change in Europe, 2001–2021, quantified using Landsat data archive. Remote Sens. Environ. 298, 113797. https://doi.org/10.1016/j.rse.2023.113797

Viana-Soto, A., Senf, C., 2025. The European Forest Disturbance Atlas: a forest disturbance monitoring system using the Landsat archive. Earth Syst. Sci. Data 17, 2373–2404. https://doi.org/10.5194/essd-17-2373-2025

Wermelinger, B., Seifert, M., 1999. Temperature-dependent reproduction of the spruce bark beetle *Ips typographus*, and analysis of the potential population growth. Ecol. Entomol. 24, 103–110. https://doi.org/10.1046/j.1365-2311.1999.00175.x

Weynants, M., Ji, C., Linscheid, N., Weber, U., Mahecha, M.D., Gans, F., 2024. Dheed: an ERA5 based global database of dry and hot extreme events from 1950 to 2022. Earth Syst. Sci. Data Discuss. 1–31. https://doi.org/10.5194/essd-2024-396

Zweifel, R., Pappas, C., Peters, R.L., Babst, F., Balanzategui, D., Basler, D., Bastos, A., Beloiu, M., Buchmann, N., Bose, A.K., Braun, S., Damm, A., D'Odorico, P., Eitel, J.U.H., Etzold, S., Fonti, P., Rouholahnejad Freund, E., Gessler, A., Haeni, M., Hoch, G., Kahmen, A., Körner, C., Krejza, J., Krumm, F., Leuchner, M., Leuschner, C., Lukovic, M., Martínez-Vilalta, J., Matula, R., Meesenburg, H., Meir, P., Plichta, R., Poyatos, R., Rohner, B., Ruehr, N., Salomón, R.L., Scharnweber, T., Schaub, M., Steger, D.N., Steppe, K., Still, C., Stojanović, M., Trotsiuk, V., Vitasse, Y., von Arx, G., Wilmking, M., Zahnd, C., Sterck, F., 2023. Networking the forest infrastructure towards near real-time monitoring – A white paper. Sci. Total Environ. 872, 162167. https://doi.org/10.1016/j.scitotenv.2023.162167